



# Revisiting and redefining return rate for determination of the precise growth status of a species

Ayan Paul<sup>1</sup> · Neelakshi Chatterjee<sup>2</sup> · Sabyasachi Bhattacharya<sup>1</sup>

Received: 5 June 2022 / Accepted: 27 January 2023 / Published online: 22 March 2023  
© The Author(s), under exclusive licence to Springer Nature B.V. 2023

## Abstract

Growth curve models play an instrumental role in quantifying the growth of biological processes and have immense practical applications across all disciplines. The most popular growth metric to capture the species fitness is the “Relative Growth Rate” in this domain. The different growth laws, such as exponential, logistic, Gompertz, power, and generalized Gompertz or generalized logistic, can be characterized based on the monotonic behavior of the relative growth rate (RGR) to size or time. Thus, in this case, species fitness can be determined truly through RGR. However, in nature, RGR is often non-monotonic and specifically bell-shaped, especially in the situation when a species is adapting to a new environment [1]. In this case, species may experience with the same fitness (RGR) for two different time points. The species precise growth and maturity status cannot be determined from this RGR function. The instantaneous maturity rate (IMR), as proposed by [2], helps to determine the correct maturity status of the species. Nevertheless, the metric IMR suffers from severe drawbacks; (i) IMR is intractable for all non-integer values of a specific parameter. (ii) The measure depends on a model parameter. The mathematical expression of IMR possesses the term “carrying capacity” which is unknown to the experimenter. (iii) Note that for identifying the precise growth status of a species, it is also necessary to understand its response when the populations are deflected from their equilibrium position at carrying capacity. This is an established concept in population biology, popularly known as the return rate. However, IMR does not provide information on the species deflection rate at the steady state. Hence, we propose a new growth measure connected with the species return rate, termed the “reverse of relative of relative growth rate” (henceforth, RRRGR), which is treated as a proxy for the IMR, having similar mathematical properties. Finally, we introduce a stochastic RRRGR model for specifying precise species growth and status of maturity. We illustrate the model through numerical simulations and real fish data. We believe that this study would be helpful for fishery biologists in regulating the favorable conditions of growth so that the species can reach a steady state with optimum effort.

**Keywords** Relative growth rate · Instantaneous maturity rate · Reverse of relative of relative growth rate · Unification · Asymptotic distribution · Stochasticity

---

✉ Sabyasachi Bhattacharya  
sabyabhattacha@gmail.com

Extended author information available on the last page of the article

## 1 Introduction

Any species' relative growth rate (henceforth, RGR) is instrumental in quantifying its underlying growth dynamics. RGR is the signature of the species fitness for several stages of the life span. RGR is a measure of identifying the species fitness within a current time window. It fails to provide any information about the maturity status of the species yet to achieve. So, the RGR function cannot determine the species precise growth and maturity status.

Recently Chakraborty et al. [2] proposed a new growth metric, i.e., instantaneous maturity rate (henceforth, IMR), to capture both the species current growth rate within a time interval and cumulative growth rate yet to achieve for the maturity. But, IMR suffers from some severe drawbacks, viz. (i) The analytical expression of IMR is not available for all the growth equations. So, it would be impossible to provide the complete growth status if any species follows a growth law, which has no explicit form of IMR. (ii) The measure of IMR depends on a model parameter. The mathematical expression of IMR possesses the term "carrying capacity," which is unknown to the experimenter. (iii) Note that for identifying the precise growth status of a species, it is also necessary to understand its response when the populations are deflected from their equilibrium position at carrying capacity. This is an established concept in population biology, popularly known as the return rate. But, IMR does not provide any information on the species deflection rate at the steady state. So, it is necessary to develop an alternative growth measure to overcome the above shortcomings of IMR. So, to explore the possibility of a more realistic growth rate, we need to know the clear definition of RGR, IMR, and return rate.

The RGR of a species is defined as the average relative growth rate, given by  $\frac{\ln(N(t_2)) - \ln(N(t_1))}{t_2 - t_1}$  for a time interval  $(t_1, t_2)$ ;  $t_2 > t_1$  with the population size  $N(t)$  [3]. We assume the interval  $(t_1, t_2)$  for notational and mathematical simplicity and considered  $(t_1, t_2)$  as  $(t, t + \Delta t)$ . We use the notation  $m(t)$  to designate the IMR for the interval  $(t, t + \Delta t)$ . More specifically, this scale invariant measure is the ratio of the two quantities. The numerator is the relative growth rate in the interval  $[t, t + \Delta t]$ , and the denominator denotes the cumulative relative growth rate (henceforth, CRGR) required to reach the asymptotic size [2]. The CRGR defines as the total fitness required to reach the carrying capacity of the cohort [2]. This measure can be empirically estimated with a discretized version which can be expressed as the ratio of Fisher's RGR [3, 4] and cumulative Fisher's RGR yet to achieve. Alternatively, IMR can also be mathematically expressed as the ratio of relative growth rate and the log difference between the current size and carrying capacity of the cohort.

The functional form of the return rate (henceforth, RR) explains the relationship between the RGR and the log density of the population size, i.e.,  $\log N(t)$ . The analytical form suggests that the measure return rate can be estimated by the slope of RGR vs.  $\log N(t)$ , at the carrying capacity. Now, to provide the precise growth status, it is necessary to observe the behavior of the growth measure around the carrying capacity of any species. RR can provide the behavior of the species growth rate around the steady state. But to understand the complete growth rate trajectory, it is essential to explore the RR for all the intermediate size values of the species in between the initial and carrying capacity of the cohort. This extended concept of return rate can be seen as the relative of relative growth rate.

Moreover, stochasticity is one of the influencing factors that can change the return rate at any population size. So, in this article, we have three folds of objectives, (i) to propose an alternative growth measure that would be able to portray the complete growth status; (ii) to revisit the return rate concept and redefine it for all the intermediate size values; (iii) and finally estimating the actual growth status of the species under the light of the

stochastic environment. Now, we organize the rest of the manuscript in the following way: First, we develop Sect. 2 to describe the utility of the recently proposed metric IMR. Next, we discuss our proposed growth measure in the subsequent Sect. 3. We also include the unification of the broad family of growth curve models by our proposed measure in Sect. 4. The asymptotic properties along with the simulation experiment are being illustrated in Sects. 5 and 6 respectively. Finally, we explain the applicability of our proposed measure in Sect. 7, and present our conclusions in Sect. 8.

## 2 Utility of IMR: a case study

In most of the cases [7–13], the modeling expert and the experimental scientists assumed the species fitness to be a decreasing function of growth. The variability of the environment obliges any species to adapt a new ecosystem by changing its fitness for its sustainability. Consequently, the fitness of the species will no longer decrease continuously with increasing its age or size. That means the fitness function deviates from the classical RGR profiles (logistic, Gompertz). It has been explored from the study of Bhowmick and Bhattacharya [1] and Chakraborty et al. [6]. The authors mentioned that the adaptability of any species depends mainly on the two yardsticks, i.e., their endogenous changes and, of course, due to the environmental changes. Due to these physiological means, initially, the fitness of the species shows an increasing trend with its age. After achieving the maximum fitness, the RGR profile decreases to zero on increasing their age (see Fig. 1a). Such a non-monotonic structure leads to the same fitness level at two distinct phases of the species life span. It will highlight the need for a new growth measure, which will provide the precise growth status of any species irrespective of their physiological changes.

The graphical pattern in Fig. 1a depicts that initially, the fitness of the species increases along the direction *AE*. However, the RGR value decreases along *EB* by attaining its maximum at point *E*. Here we consider a horizontal (red) line *AB* (see Fig. 1a) representing the

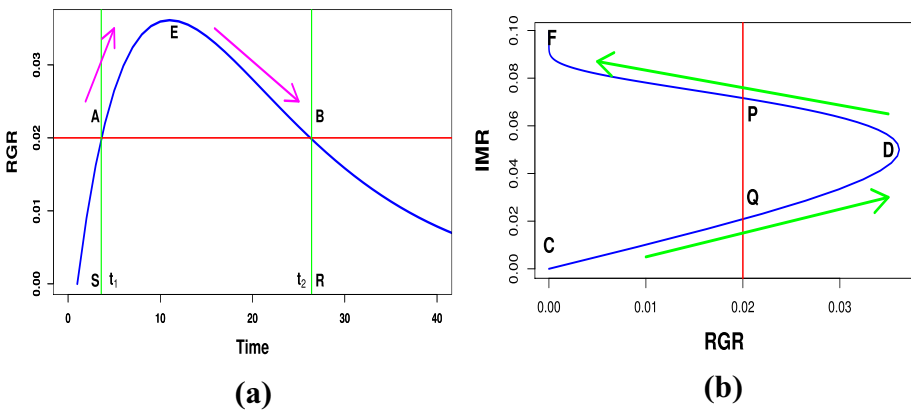


**Fig. 1** The sub-figure (a) shows that adaptability in the new environment leads any species to a bell-shaped RGR profile so that species can achieve the same amount of fitness at two different time points [1, 5, 6]. The sub-figure (b) ensured the parabolic-shaped structure between species fitness and the IMR. At a particular amount of species fitness, their maturity rate differs significantly

same level of fitness at two distinct stages of the species life cycle. For convenience, we contemplate the two different time points by  $t_1$  and  $t_2$ . Note that the time point  $t_1$  indicates the earlier stage of the species growth process, i.e., before gaining the maximum fitness. However, another phase of the growth cycle is denoted by the time point  $t_2$ , where the species are on the verge of maturity. More precisely, the vertical solid (green) line through the point  $A$  in Fig. 1a is the fitness level at the earlier stage of the species growth cycle, i.e., at the time  $t_1$ . We denote the fitness level during the time  $t_2$  by the vertical solid (green) line passing through the point  $B$ . Despite having two different stages of life at  $t_1$  and  $t_2$ , the fitness levels of the species at these distinct time points are the same. This may lead to one relationship between the species age with its fitness leads us to select a new metric to conclude the accurate growth status of the species.

In this connection, we opt for the measure IMR proposed by Chakraborty et al. [2] to deliver a precise growth status of the species which are subjected to the adaptation. It is worthy of mentioning that the scale invariant measure IMR has the following functional relationship,

$$\text{IMR}(t) = \frac{R(t)}{\int_t^\infty R(u)du} = \frac{RGR}{CRGR}. \quad (1)$$

Here,  $R(t) = \frac{1}{N(t)} \frac{dN(t)}{dt}$  denotes the RGR value for any population size  $N(t)$  at any instantaneous time point  $t$ . The application of this new growth metric gives a new dimension to the non-monotonic fitness function, which is presented in Fig. 1b. The diagram elucidates the variation of IMR according to the change in RGR values. It is worth mentioning that the IMR profile regarding the RGR function possesses two branches, i.e.,  $CD$  and  $DF$ . The relationship initially traces the path  $CD$ , then follows the reverse direction, i.e.,  $DF$ . The distinction of the IMR graph into two branches generates two points,  $P$  and  $Q$ . These two points lie in the same vertical (red) line with the fixed RGR value. That means for a certain fitness level, Fig. 1b is enabled to provide two distinct IMR values, which can portray the species maturity states in a better way. We observe that at position  $A$ , the species have to gain more fitness to reach their maturity, which yields a lower amount of IMR value, i.e., the stage  $Q$ . Consequently, the magnitude of IMR will be higher than the previous case, i.e., the point  $P$  when the species growth stage is designated by the coordinate  $B$  as they will cover a low amount of fitness to attain the matured stage. So, the points  $P$  and  $Q$  are contemporary with  $B$  and  $A$ , respectively, due to the same fitness value say,  $r^*(= 0.02 \text{ time}^{-1}$  in Fig. 1). So, the horizontal (red) line  $AB$  is mapped into the vertical (red) line  $QP$ . Hence, IMR can provide the precise growth information of the species instead of RGR.

Note that such a non-monotonic fitness structure does not follow the classical RGR growth equations, viz. logistic, extended logistic, Gompertz, etc. In this connection, Bhowmick and Bhattacharya (2014) [1] propose a new growth curve model, popularly known as the Bhowmick-Bhattacharya extended Gompertz model (henceforth, BBEGM), which can cover this type of RGR profile. The analytical expression of that growth model is

$$R(t) = \frac{1}{N(t)} \frac{dN(t)}{dt} = be^{-at}t^c, \quad (2)$$

with  $b$ ,  $a$ , and  $c$  denote the growth rate, decay rate, and adaptability parameter respectively. Since RGR is unable to provide precise growth information, one needs to evaluate the closed form expression of IMR for the new growth model BBEGM, which is absent in the research work of Chakraborty et al. [2] due to the mathematical complexity. A detailed discussion about the shortcomings is presented in Sect. 7. Moreover, any enclosed populations have the

basic characteristics to return to their steady state due to the application of the small perturbations. The rate at which the species returns is termed as ‘‘Return rate’’ [14]. The measure is used in conserving any species when they are subjected to any external perturbations [15]. The IMR is also unable to provide a spotlight on the species return rate too. So, there is an urge to propose a new metric that can overcome these difficulties and provide substantial information for nurturing the species growth process in a better way.

### 3 Return rate and its extension: a competitor of IMR

RGR is the growth rate of any species for a specific time window with the current population size. Also, the RGR function has the characteristic that it does not depend on any information about the whole growth process or the asymptotic size. However, the experimenter needs to know how much RGR is necessary for a species to reach the usual size at any time point. Keeping this in mind, Chakraborty et al. [2] propose a new growth metric IMR,  $m(t)$  to provide the information on the species maturity status at any time point  $t$ . Note that the analytical expression of IMR in Eq. 1 possesses an alternative form, which is given by

$$m(t) = \frac{R(t)}{\ln(K) - \ln(N(t))}, \tag{3}$$

where  $K$  denotes the cohort’s carrying capacity or asymptotic size, as most species have an intrinsic property to spend their maximum lifetime around their carrying capacity. However, any population should reach its asymptotic size at the mature stage, and hence the RGR value vanishes. Species attain their highest maturity at the large time interval of the entire growth cycle. So, both the numerator and denominator of the right-hand side of Eq. 3 become zero at the large time point. This theoretical concept gives the brainchild of a new growth metric. Hence, the mathematical simplicity turns the expression of IMR in Eq. 3 into the following form

$$\lim_{t \rightarrow \infty} m(t) = \lim_{t \rightarrow \infty} \frac{R(t)}{\ln K - \ln(N(t))} \left[ \frac{0}{0} \text{form} \right]. \tag{4}$$

Since both the RGR function ( $R(t)$ ) and population size ( $N(t)$ ) have the first-order continuous derivatives so, the application of the famous L’Hospital rule on the above expression will become

$$\begin{aligned} \lim_{t \rightarrow \infty} m(t) &= \lim_{t \rightarrow \infty} \frac{R(t)}{\ln K - \ln(N(t))} \\ \implies \lim_{t \rightarrow \infty} m(t) &= \lim_{t \rightarrow \infty} \left[ -\frac{1}{R(t)} \frac{dR(t)}{dt} \right] \\ \therefore m(t) &\sim -\frac{1}{R(t)} \frac{dR(t)}{dt} \text{ for the large time point.} \end{aligned} \tag{5}$$

We treat the expression  $-\frac{1}{R(t)} \frac{dR(t)}{dt}$  as the new growth measure, which can be termed as the ‘‘Reverse of Relative of Relative growth rate’’ (henceforth, RRRGR). For the notational simplicity, we denote the metric RRRGR by  $\omega(t)$ . Since  $m(t)$  and  $\omega(t)$  are indistinguishable at the large time window, one can use RRRGR as the proxy measure of the IMR.

### 3.1 RR and RRRGR are equivalent

In general, when the population size is small, the resource is abundant, and the species have sufficient support of food, shelter, and habitat. Naturally, the fitness of the species is high. When the population reaches carrying capacity, the resource is exhausted. Consequently, the species fitness is reduced. But at the same time, the small population is more sensitive to the perturbations. How much a population is affected temporarily by the deflection will be an opposite function of the species fitness. Hence, there is a possibility that the small population may not return to its original size, but a minor disturbance does not affect the population at all when the size of the density is large or the population is reached a steady state. Hence, the return rate and RRRGR are showing the equivalent properties.

The return rate of any species is defined as the rate at which the population will return to its steady state after deflecting from its stable equilibrium point, i.e., carrying capacity [14–16]. May et al. [14] first coined the term and shows the utility of RR in measuring the species stability. RR can be estimated as the slope of the relationship between RGR and log density at the carrying capacity of the species, which is given by,

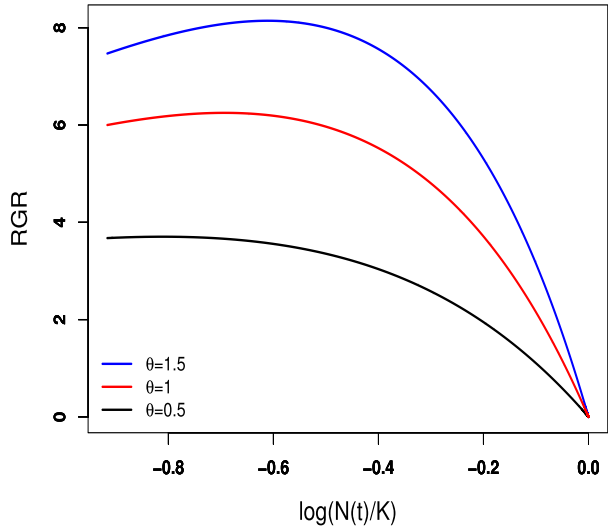
$$\text{return rate} = - \left[ \frac{dR(t)}{d \ln N(t)} \right]_K = \left[ - \frac{1}{R(t)} \frac{dR(t)}{dt} \right]_K. \quad (6)$$

The above mathematical form demonstrates that to estimate RR, the species have to reach its asymptotic size ( $K$ ). Although this structural form is expressed as the rate of change of RGR to the log size of the population density, the functional relationship of RR can highlight another important demographic trait of the species growth cycle. That demographic characteristic can be elucidated by the negative RGR of RGR at the species carrying capacity. RR measures the species deflection rate at its asymptotic size and enumerates the relative fitness value at the steady state of any species. Our proposed growth metric RRRGR has a structural similarity with the measure RR. The relationships 5 and 6 show that RRRGR becomes identical with RR at the steady state of any species. So, applying the metric RRRGR not only quantifies the growth profile but also measures the deflection rate just like RR at each population density throughout the species growth process. So, by applying the RRRGR measure, we can estimate the return rate of species at any size  $N(i)$  for the time point  $i$ . Here, we explain this situation by the theta-logistic model [12] in Fig. 2a and b. The analytical form of the theta-logistic model is given by

$$\text{RGR} = R(t) = \frac{1}{N(t)} \frac{dN(t)}{dt} = r \left( 1 - \left( \frac{N(t)}{K} \right)^\theta \right). \quad (7)$$

Here  $r$ ,  $\theta$ , and  $K$  denote the intrinsic growth rate, density regulation parameter, and carrying capacity, respectively, with the population size  $N(t)$  at any time point  $t$ . The diagram shows a concave upward relationship between the RGR and  $\log N(t)/K$ . Due to the non-linear relationship, the RGR and log density rate become dynamic. Figure 2 also explains the case that if the species experiences a small perturbation at any arbitrary size  $N(i)$  at the time point  $i$ , it can stably return to its original size. The growth function RRRGR can measure this case. Hence, the proposed metric RRRGR quantifies the species growth profile and has a strong connection with the stability of the entire growth process of any species.

**Fig. 2** The relationship between the RGR and the population size is measured as  $\log(N(t)/K)$  for the theta-logistic model 7. Note that irrespective of the magnitude of the density regulation parameter, the relationship always shows a concave trait



### 4 Unification of various growth laws through RRRGR

Recently Chakraborty et al. [17] proposed a unified form of species fitness function. So, in the author’s spirit, we will provide a unified form of our proposed growth measure, i.e., RRRGR, and demonstrate how it helps to capture a large family of the existing growth curve models. The unified form of RGR is

$$R(t) = \frac{r}{b^d} y^a (1 - y^b)^d t^{c-1} \left[ \text{Here, } y \equiv y(t) = \frac{N(t)}{K} \right] \tag{8}$$

On differentiation with respect to  $t$ , we have

$$\omega(t) = -\frac{1}{R(t)} \frac{dR(t)}{dt} = \frac{1-c}{t} + \frac{r}{b^d} y^a (1 - y^b)^{d-1} [y^b(a + bd) - a] t^{c-1} \tag{9}$$

Hence, Eq. (9) is the unified form of the RRRGR for the existing growth models. Further differentiation of  $\omega(t)$  with respect to  $t$  gives

$$\frac{d\omega(t)}{dt} = \frac{c-1}{t^2} - \left[ a + \frac{bd y^b}{y^b - 1} \right] \frac{dR(t)}{dt} + \frac{R^2(t) b^2 d y^b}{(y^b - 1)^2} \tag{10}$$

#### 4.1 Tsoularis and Wallace model

According to the unified form of the species fitness (i.e., Eq. 8), the expression of RGR for the Tsoularis and Wallace growth model [10] is obtained by putting  $c = 1$  in that equation. Therefore, the expression for the RRRGR is

$$\omega(t) = \frac{r}{b^d} y^a (1 - y^b)^{d-1} [y^b(a + bd) - a] \tag{11}$$

and from the expression 10 we again get that

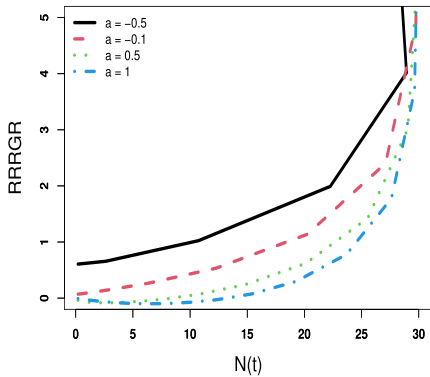
$$\frac{d\omega(t)}{dt} = - \left[ a + \frac{bdy^b}{y^b - 1} \right] \frac{dR(t)}{dt} + \frac{R^2(t)b^2d y^b}{(y^b - 1)^2} \tag{12}$$

Here the second term on the right-hand side is always positive but on the first term the positivity of  $\frac{dR(t)}{dt}$  depends on some condition. Chakraborty et al. [17] shows that  $\frac{dR(t)}{dt} > 0$  if  $0 \leq y \leq \left(\frac{a}{a+b}\right)^{\frac{1}{b}}$ . Considering this it can be shown that  $\frac{d\omega(t)}{dt}$  should be positive if the relation  $a \leq bd$  holds. Hence, RRRGR should be an increasing function for  $a \leq bd$ .

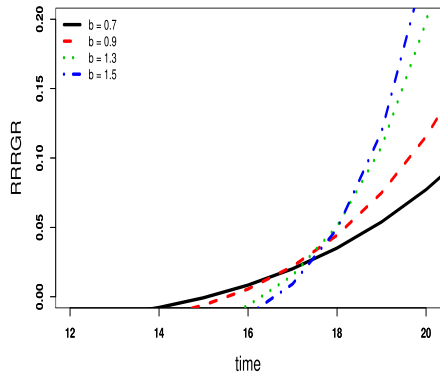
### 4.1.1 Marusic-Bajzer growth model ( $d = 1$ )

Since Marusic-Bajzer growth law [18] follows from the Tsoularis and Wallace model [10], so the shape of RRRGR must be increasing for the relation  $a \leq b$  and that of decreasing for  $a > b$ . The various forms of the graph are given in Fig. 3a, b.

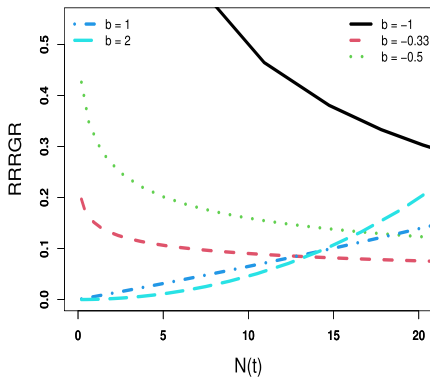
Chakraborty et al. [17] show that the Richard growth curve model [9] can be obtained by putting  $a = 0$  and  $b \geq -1$  in Eq. (8). Moreover, the Monomolecular growth law [17] with  $b = -1$ ,  $r < 0$ ; General Von Bertalanffy model with  $0 < b < 1$ ,  $r < 0$ ; Von



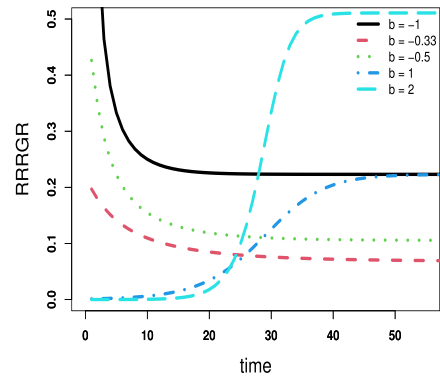
(a) Marusic-Bajzer growth law ( $b = 1, d = 1$ )



(b) Marusic-Bajzer growth law ( $a = 0.2, d = 1$ )



(c) Richards growth model ( $a = 0, d = 1$ )



(d) Richards growth model ( $a = 0, d = 1$ )

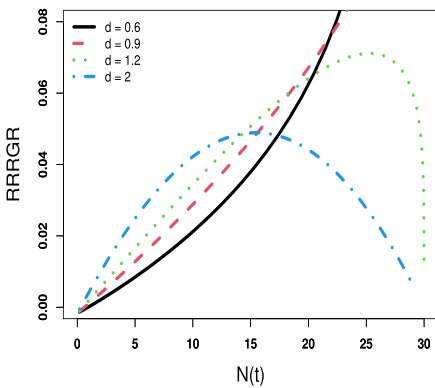
**Fig. 3** The sub-figure (a), (b) denote the shapes of RRRGR profile for the Marusic-Bajzer growth laws, whereas the sub-figures (c), (d) indicate several shapes of RRRGR for the Richards law with respect to size and time respectively



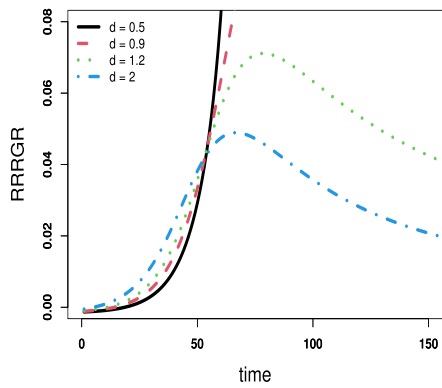
Bertalanffy with  $b = -\frac{1}{3}, r < 0$  [19]; logistic with  $b = 1$  [7]; and Gompertz with  $b \rightarrow 0$  [8] are cited as the special case of the Richard growth curve family. Among which the shape of the RRRGR of the first 3 members i.e. the Monomolecular growth law, General Von Bertalanffy model, and Von Bertalanffy take the decreasing pattern but in the case of logistic and Gompertz the shape should be increasing. This scenario is depicted in Fig. 3c, d for various values of  $b$ .

### 4.1.2 Blumberg growth model ( $b = 1$ )

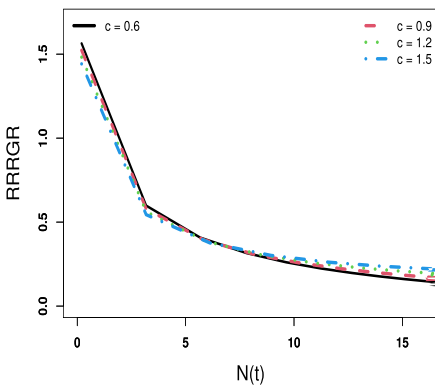
Blumberg’s growth law [20] is also a generalization form of the Tsoularis-Wallace growth model [10] which is obtained by replacing the parameter  $b$  by 1. Note that RRRGR of the Blumberg growth model also follows the decreasing trend by maintaining the relation  $a \geq d$  along with the increasing pattern for the relation  $a < d$  but it is observed that, due to the functional form of the RGR equation, the Blumberg growth law also shows some bell-shaped structure for  $a < d$ . All of these different traits are presented in Fig. 4a, b.



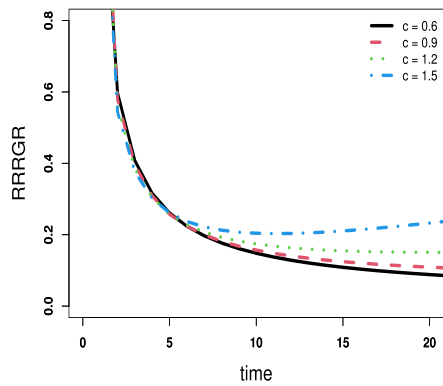
(a) Blumberg growth law ( $r = 0.1, a = 0.02$ )



(b) Blumberg growth law ( $a = 0.02, r = 0.1$ )



(c) Weibull model ( $r = 0.1$ )



(d) Weibull model ( $r = 0.1$ )

**Fig. 4** The sub-figure (a), (b) denote the shapes of RRRGR profile for the Blumberg growth laws, whereas the sub-figures (c), (d) indicate several shapes of RRRGR for the Weibull growth models with respect to size and time respectively.

### 4.1.3 Generalized Gompertz model ( $a = 0, b \rightarrow 0$ )

As mentioned above, the relative fitness function takes the decreasing pattern for the relation  $a \geq bd$ . Since for the generalized Gompertz the parameter  $a$  takes zero value and both  $b$  and  $d$  being positive real number, so it clearly implies that the pattern of the relative fitness function should be increasing. But on the special case i.e. for the Gompertz law [8] RRRGR should be a constant and it is exactly equal to the species intrinsic growth rate. Another special case of this growth law is the second-order exponential model ( $d = \frac{1}{2}$ ) and in this case the RRRGR function is as usual follows the increasing pattern.

### 4.1.4 Generic model ( $a = b(1 - d)$ )

Generic model [21] is also another special case of the Tsoularis and Wallace model [10]. Therefore, the relative fitness profile shows a decreasing pattern for the relation  $a \geq bd$  i.e. in this case  $d \leq \frac{1}{2}$ . But, this condition is not enough for justifying the decreasing or increasing pattern of the RRRGR function due to the presence of the function  $\frac{dR(t)}{dt}$  in  $\frac{d\omega(t)}{dt}$  (10). In the above discussed growth model, this phenomena did not happen because any of the parameter takes either zero or the value 1.

In order to follow the increasing pattern, the required condition is  $d \leq 1$  and  $\frac{dR(t)}{dt} \leq 0$ . Chakraborty et al. [17] show that RGR for generic model would be decreasing if  $\left(\frac{a}{a+b}\right)^{\frac{1}{b}} \leq y \leq 1$ . Following this condition, we get that relative fitness shows increasing pattern for  $\left(\frac{b(1-d)}{2b-2d}\right)^{\frac{1}{b}} \leq y \leq 1$  and it will show a decreasing trend for  $0 \leq y \leq \left(\frac{b(1-d)}{2b-2d}\right)^{\frac{1}{b}}$  along with  $d > 1$ .

## 4.2 Korf model

The Korf model [22] is followed from the unified equation of RGR (8) by putting  $a = 0, d = 0, c < 0$ . Therefore,  $\frac{d\omega(t)}{dt} = \frac{c-1}{t^2}$ . Since  $c < 0$  so it implies that  $\frac{d\omega(t)}{dt} < 0$ . Therefore, the relative fitness of any species under the Korf model follows a decreasing trend always.

## 4.3 Koya-Goshu model

Chakraborty et al. [17] show that from Eq. (8) the RGR of the Koya-Goshu model [23] can be expressed in multiple ways depending on the choice of the parameter  $a, b$ . Note that the parameter  $d$  is always 1 for this model. One of the standard form is obtained by considering the parameter  $a = 0$  and  $b < 0$ . In this case, the expression for the RRRGR is

$$\omega(t) = \frac{1-c}{t} - \frac{by^b}{y^b-1}R(t) \quad (13)$$

and,

$$\frac{d\omega(t)}{dt} = \frac{c - 1}{t^2} - \left[ a + \frac{bdy^b}{y^b - 1} \right] \frac{dR(t)}{dt} + \frac{R^2(t)b^2dy^b}{(y^b - 1)^2} \tag{14}$$

Since  $b < 0$ ,  $y^b - 1 < 0$ , and for  $c \leq 1$ , Chakraborty et al. [17] show that  $\frac{dR(t)}{dt}$  is negative so combining all of these things we can say that  $\frac{d\omega(t)}{dt}$  is also negative. This clearly implies that for  $c \leq 1$  RRRGR function is decreasing and in a similar way we can show that for  $c > 1$  the species relative fitness should be increasing.

### 4.3.1 Weibull model

The RGR of the Weibull growth model [24] can be obtained by considering the parameter  $a$  as  $-1$ ,  $b$ , and  $d$  as  $1$  in the unified RGR Eq. (8). In a similar way, the expression for the RRRGR is

$$\omega(t) = \frac{1 - c}{t} + ry^{-1}t^{c-1}. \tag{15}$$

and similarly from (10) we get that,

$$\begin{aligned} \frac{d\omega(t)}{dt} &= \frac{c - 1}{t^2} - \frac{1}{y - 1} \frac{dR(t)}{dt} + \frac{R^2(t)y}{(y - 1)^2} \\ &= \frac{c - 1}{t^2} + \frac{1}{y - 1} \left[ \frac{R^2(t)y}{y - 1} - \frac{dR(t)}{dt} \right]. \end{aligned} \tag{16}$$

Therefore, the following two cases will arise:

- The first term on the right-hand side of the above expression (16) will be negative if  $c < 1$ . But to maintain the negativity of  $\frac{d\omega(t)}{dt}$ , one extra condition is that  $y < \frac{r^c}{c - 1 + r^c}$ .
- Moreover for  $c > 1$ , the function  $\frac{d\omega(t)}{dt}$  is also negative if

$$\frac{c - 1}{t} \left[ \frac{1}{t} + ry^{-1}(1 - y)t^{c-1} \right] < r^2y^{-2}(1 - 2y)t^{2c-2}$$

Hence, it is quite clear that, for both the cases i.e. for  $c < 1$  and for  $c > 1$ , RRRGR of Weibull model should be decreasing. All possible shapes are provided in Fig. 4c, d.

### 4.3.2 Extended Gompertz model

The RGR of the extended Gompertz growth law [6] can be expressed as

$$R(t) = r(-lny) t^{c-1} \tag{17}$$

Therefore, the expression of RRRGR is given as

$$\omega(t) = r t^{c-1} - \frac{c - 1}{t} \tag{18}$$

and on differentiation with respect to  $t$  we have

$$\frac{d\omega(t)}{dt} = (c - 1) \left[ r t^{c-2} + \frac{1}{t^2} \right] \tag{19}$$

It is quite clear that,

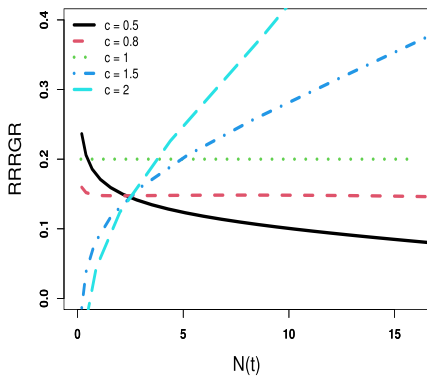
- If  $c < 1$ ,  $\frac{d\omega(t)}{dt} < 0$  which implies that  $\omega(t)$  must be a decreasing function of size and time both.
- If  $c > 1$ ,  $\frac{d\omega(t)}{dt} > 0$  which implies that  $\omega(t)$  must be an increasing function of size and time both.

The possible shapes of RRRGR are given in Fig. 5a, b.

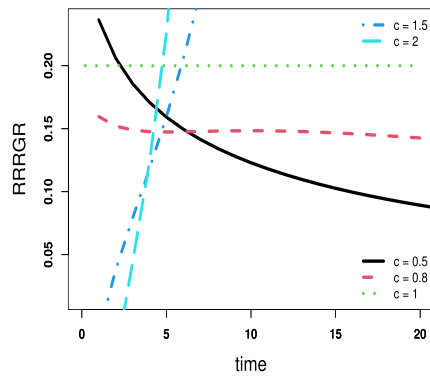
### 4.3.3 Extended logistic model

Chakraborty et al. [6] proposed an extended version of the logistic growth law popularly known as the proposed extended logistic model (PELM). The fitness function of this growth model is described as

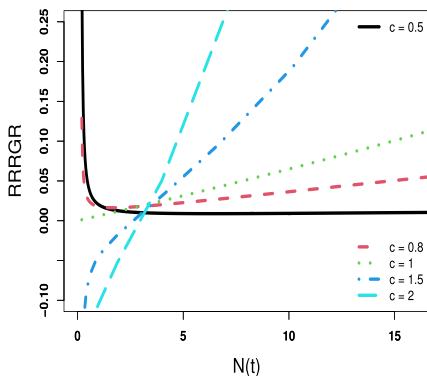
$$R(t) = r(1 - y)t^{c-1} \tag{20}$$



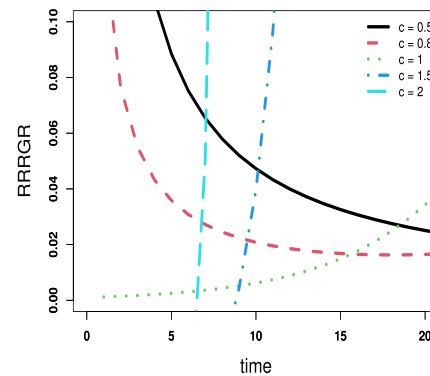
(a) Extended Gompertz growth law ( $r = 0.2$ )



(b) Extended Gompertz growth law ( $r = 0.2$ )



(c) Extended logistic growth law ( $r = 0.2, K = 30$ )



(d) Extended logistic growth law ( $r = 0.2, K = 30$ )

**Fig. 5** The sub-figure (a), (b) denote the shapes of RRRGR profile for the Extended Gompertz growth laws, whereas the sub-figures (c), (d) indicate several shapes of RRRGR for the Extended logistic growth models with respect to size and time respectively

Hence from Eq. (8), the RRRGR expression for this growth is,

$$\omega(t) = r y t^{c-1} + \frac{1-c}{t} \tag{21}$$

and on differentiation with respect to  $t$

$$\frac{d\omega(t)}{dt} = r y t^{c-1} \left[ R(t) + \frac{c-1}{t} \right] + \frac{c-1}{t^2} \tag{22}$$

It is quite clear that if  $c > 1$  holds, the relative fitness function must be increasing and for  $c < 1$  the RRRGR function follows the decreasing pattern. The possible shapes are included in Fig. 5c, d.

**Remark 1** The analytical expression of the RRRGR for a broad family of growth models is available in Table 1 of the supplementary material. We also prepare Table 1 to compare the shape of RGR and RRRGR functions for the mentioned growth models. Figures 6 and 7 also illustrate the pattern of the RRRGR functions for the broad family of growth laws according to the population size and time, respectively. However, the closed form expression of the size variable for the cooperation model [25] and BBEGM [1] does not exist. Consequently, the analytic form of IMR is intractable for these growth models. In this connection, we prepare the table to incorporate the RGR and RRRGR expressions for both the mentioned growth laws and the asymptotic values of our proposed growth measure. The table is available in the supplementary file.

**Table 1** Classification of growth curves with their shapes. Here, the notations  $I, D, B,$  and  $U$  represent the increasing, decreasing, bell-shaped, and bath-tub trends

Srl.	Growth models	Shape of RGR over size	Shape of RRRGR over size
1	Exponential	C	C
2	Power	I	D
3	Logistic	D	I
4	Monomoleculer	D	D
5	Richards	D	I
6	Gompertz	D	C
7	Generalized Gompertz	D	$I_{d < 1}, D_{d > 1}$
8	Second-order exponential polynomial	D	I
9	Von Bertalanffy	D	D
10	Generalized Von Bertalanffy	D	D
11	Weibull	D	D
12	Tsoularis and Wallace	$D_{a \leq 0}, B_{a > 0}$	$D_{a > 0}, U_{a < 0}$
13	Korf	D	$D_{c < 1}, I_{c > 1}$
14	Extended logistic	$B_{c > 1}, D_{c \leq 1}$	$I_{c > 1}, D_{c < 1}$
15	Extended Gompertz	$B_{c > 1}, D_{c \leq 1}$	$I_{c > 1}, D_{c < 1}$
16	Marusic and Bajzer's	$D_{a \leq 0}, B_{a > 0}$	-
17	Blumberg	$D_{a \leq 0}, B_{a > 0}$	$I_{d \leq 1}, B_{d > 1}$
18	Generic	$B_{d < 1}, D_{d \geq 1}$	-
19	Hyperbolic	D	D
20	Koya-Goshu model ( $b < 0$ )	$B_{c > 1}, D_{c \leq 1}$	$I_{c > 1}, D_{c < 1}$

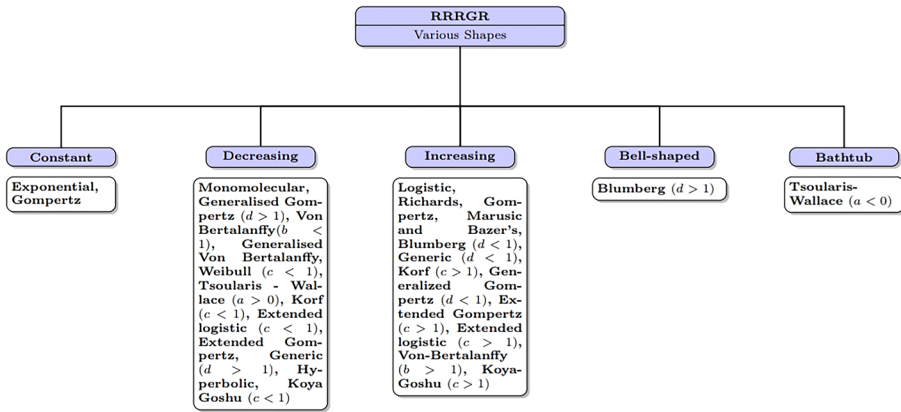


Fig. 6 Classification of various growth curves according to the shapes of RRRGR to the population density

**Remark 2** Like the RGR and IMR, the proposed measure RRRGR can also be identified by its shape and population size or time. Since RRRGR is an alternative form of IMR, in most cases, the behavior of  $\omega(t)$  should be similar to  $m(t)$ . For example, the shape of the RGR function for the Richard law [9] is decreasing in Fig. 8a, b; though the shape of the RRRGR profile has the monotonic increasing structure in Fig. 8c, d. We also observe in Fig. 9a, b that the RGR profiles are showing a decreasing pattern, but the RRRGR functions are constant for the Gompertz law [8] (see Fig. 9c, d). Note that IMR also has the same property for these two growth curve models. Hence, unlike the IMR, the metric RRRGR can also be used as the characterization growth response function to identify the true underlying model.

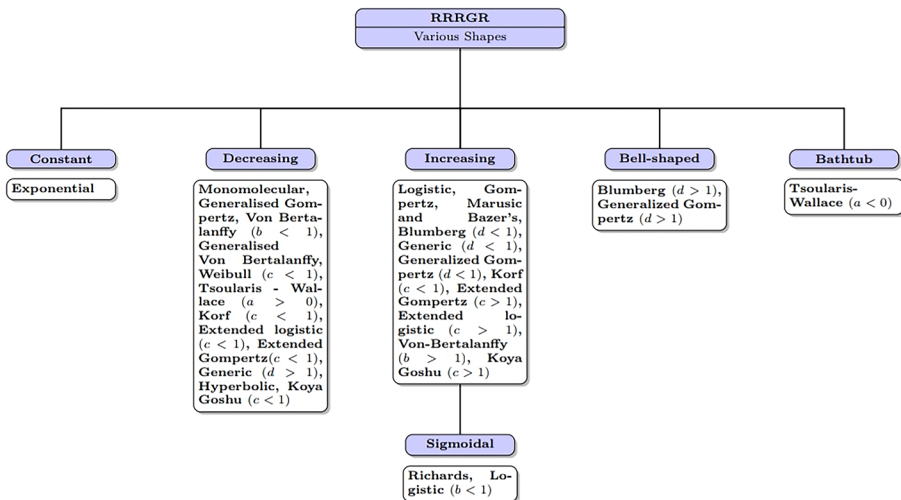
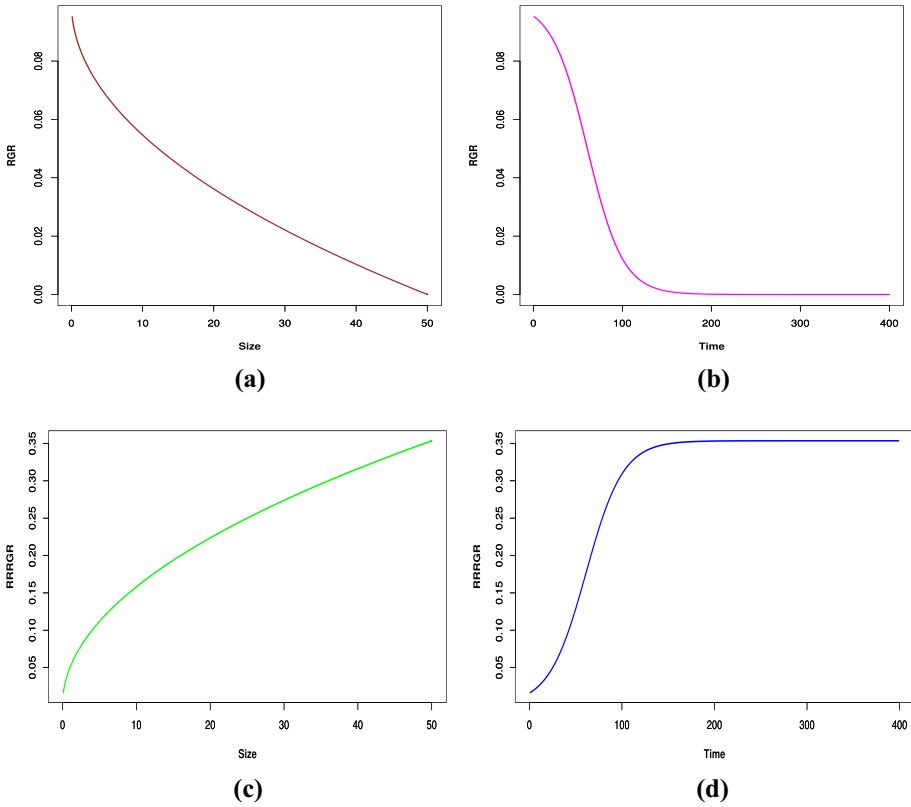


Fig. 7 Classification of various growth curves according to the shapes of RRRGR to the time



**Fig. 8** The plot of the Richard growth law ( $b < 1$ ) [9] over size and time. The first column (sub-figure a, c) denotes the profile of the RGR and RRRGR over size, whereas the second column (sub-figure b, d) indicates the same over time. The diagram reflects that although the trait of the RGR profile is decreasing for the Richard growth law [9], the trend of the RRRGR function shows an increasing character

**Remark 3** Despite having such similarities, some growth laws still exist for which a distinction is observed in the shape of IMR and RRRGR. In this connection, we consider two growth laws, viz. Korf [22] and Von-Bertalanffy model [19] for conducting the experiment. Figure 10a, d, and b, e illustrate that the RGR and IMR profile of both the Von-Bertalanffy [19] and Korf functions [22] are showing a decreasing trend, which is misleading for any experimenter to identify the true growth law. However, Fig. 10c and f ensure that the trait of RRRGR profile of Von-Bertalanffy law maintains the decreasing character unlike IMR, though it is not the same for the Korf growth model, since the RRRGR profile shows the monotonic increasing character for the Korf growth function (see Fig. 10f). In the subsequent section, we shall discuss the properties of the proposed measure RRRGR for a broad family of growth curves.

**Remark 4** The proposed measure RRRGR has the dimension  $\text{Time}^{-1}$ , which shows that the proposed measure has a close synergy with the frequency of any wave motion. So, depending on the RRRGR function, one can easily tune the species growth profile.

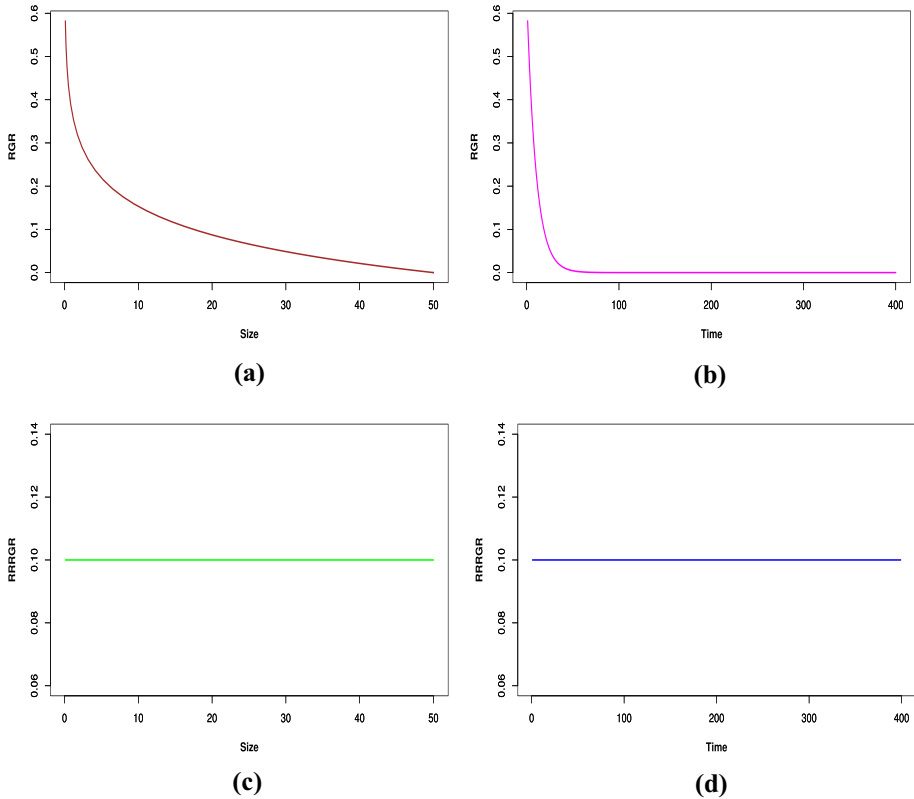


**Fig. 9** The plot of the Gompertz growth law [8] over size and time. The first column (sub-figure a, c) denotes the profile of the RGR and RRRGR over size, whereas the second column (sub-figure b, d) indicates the same over time. The diagram reflects that although the trait of the RGR profile is decreasing for the Gompertz law, the RRRGR function becomes constant

**Remark 5** Allee effect phenomenon is characterized by the increasing fitness profile of any species at its low density. The mathematical expression of the Allee growth model [26] is

$$\frac{dN(t)}{dt} = rN(t)\left(\frac{N(t)}{A} - 1\right)\left(1 - \frac{N(t)}{K}\right). \tag{23}$$

Here  $r$ ,  $K$ , and  $A$  indicate the instantaneous growth rate, carrying capacity, and Allee threshold parameters respectively. Saha et al. [27] modify Eq. (23) by introducing the concept of density dependence, which can be expressed by

$$\frac{dN(t)}{dt} = rN(t)\left(\frac{N(t)}{A} - 1\right)\left(1 - \left(\frac{N(t)}{K}\right)^\theta\right). \tag{24}$$

Note that the model (24) is popularly known as the Allee-Saha model (ASM) with  $\theta$  as the density-dependent parameter. Hence, the analytical expression of RRRGR function of the Allee growth equation is given by  $\omega(t) = rN(t) \left[ \frac{1}{1 - \frac{N(t)}{A}} + \frac{\theta N^{-1}(t)}{\left(\frac{K}{N(t)}\right)^\theta - 1} \right] \left(\frac{N(t)}{A} - 1\right)\left(1 - \left(\frac{N(t)}{K}\right)^\theta\right)$ .



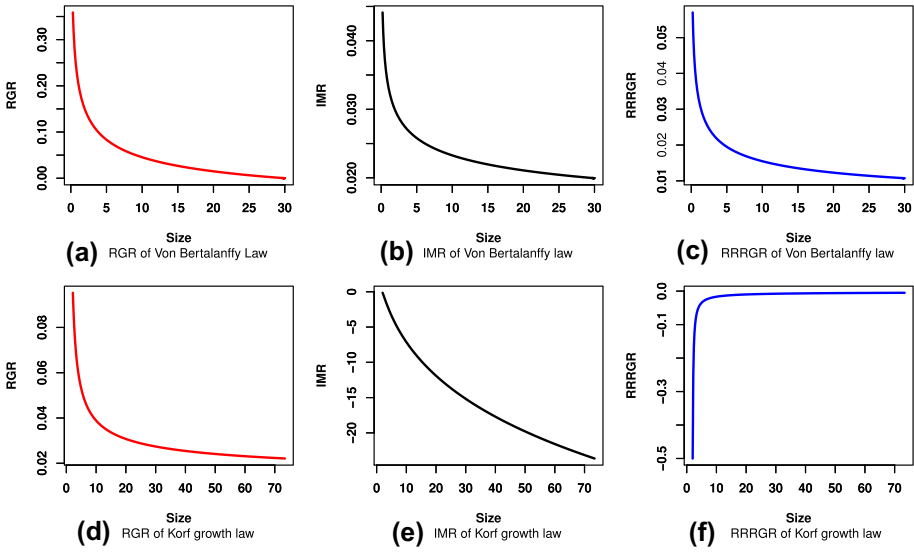


**Fig. 10** Comparison between the shape of RGR, IMR, and RRRGR profiles between Von Bertalanffy [19] and Korf model [22]. The figures (a), (b) and (d), (e) demonstrate that for both the Von Bertalanffy [19] and Korf growth model [22], the trait of the RGR and IMR follows the decreasing pattern, whereas the laws can be distinguished by their RRRGR character, which is reflected in the sub-figure (c), (f). Since the Von-Bertalanffy model [19] possesses a decreasing character, the Korf law [22] has an increasing trend for the RRRGR function

The shapes of the RRRGR function for distinct magnitudes of  $\theta$  are presented in Fig. 11a. The time series structure in Fig. 11b demonstrates the sigmoidal pattern, whereas the population size profile of Fig. 11a elucidates the U-shaped trend.

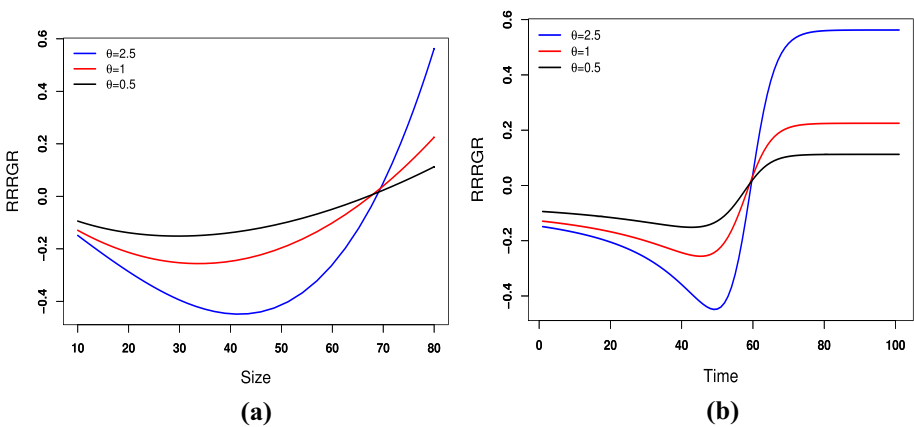


**Fig. 11** Several shapes of RRRGR profile for the extended Allee growth function (24). The different traits are generated for the distinct level of density regulation parameter, which is mentioned in the legend of the figures (a), (b). Here the unit level of density regulation indicates the Allee growth Eq. (23)

### 5 Asymptotic distribution of RRRGR

We develop this section to study the statistical properties of the empirical estimate of the proposed measure RRRGR. This kind of statistical manipulation will help to construct the likelihood functions during the parameter estimation process. Here, we use the notation  $N_t$  to distinguish a random variable whose realizations are the observed data. Moreover, we also consider  $N_t$  as the population density at time point  $t$ , where  $t = t_1, t_2, \dots, t_q$  and denote  $N = (N(t_1); N(t_2); \dots; N(t_q))'$  as the vector of the observations. Let us suppose that at each time point, we collect the data of  $n$  individuals so that we have  $n$  independent and identically distributed (iid) observations at each time point  $t_j$ , and the data matrix is thus given by:

$$N_{n \times q} = \begin{bmatrix} N_{1t_1} & N_{1t_2} & \dots & N_{1t_q} \\ N_{2t_1} & \ddots & \ddots & \vdots \\ \vdots & \ddots & \ddots & \vdots \\ N_{nt_1} & N_{nt_2} & \dots & N_{nt_q} \end{bmatrix}$$

Here  $N_{ij}$  represents the size of  $i$ -th individual at the  $j$ -th time point for  $i = 1, 2, \dots, n$  and  $j = t_1, t_2, \dots, t_q$ . It is worthy to mention that the row vectors of the matrix  $N_{n \times q}$  represent the iid of order  $q$ . Now, for the sake of convenience, let us fix any particular column of the matrix  $N_{n \times q}$ , where each component of this column vector is independent and identically distributed. In the spirit of Pal et al. [4], we also consider that each row of the data matrix  $N_{n \times q}$  follows the multivariate normal distribution, whose mean is specified by the underlying deterministic growth equation. The further assumption on the structure of the variance-covariance matrix will be explained later. In the following, we consider the extended Gompertz growth equation as a test-bed to develop the asymptotical distribution of RRRGR. Note that the methodology can be easily extended for other growth equations as well. Now, the analytical expression of the RRRGR function can be represented by,

$$\omega(t) = -\frac{1}{R(t)} \frac{dR(t)}{dt}$$

So, the estimate of RRRGR is given by

$$\begin{aligned} \widehat{\omega}(t) &= \log \left( \frac{\overline{R(t)}}{R(t+1)} \right) \\ &= \log \left[ \frac{\log \overline{N(t+1)} - \log \overline{N(t)}}{\log \overline{N(t+2)} - \log \overline{N(t+1)}} \right] \end{aligned} \tag{25}$$

**Remark 6** Here the growth observation vectors of each individual are not independent, and hence we assume multivariate normality with a specific (Koopmans) covariate structure. We assume the mean of this multivariate normal is an asymmetric growth curve, which is more realistic in population dynamics. Moreover, for a given time point, the independent growth observations of different individuals follow the normal distribution, where the mean is the realization of the Gompertz model for the same time point. So, the growth observations of the same individuals over time points are not independent, but the observation vectors for the different individuals are the independent sample from multivariate normal.

Note that the analytical expression of  $\widehat{\omega}(t)$  possesses a highly non-linear structure of the three random variables  $\overline{N}_{t_i}$  for  $i = 1, 2, 3$ , whose joint distribution is multivariate normal (hence, each  $\overline{N}_{t_i}$  has the marginal normal distribution). In this connection, we will use the following lemma [2, 4, 28, 29] to derive the required asymptotic distribution.

**Lemma 1 The multivariate delta method:** Let  $Y_n = (Y_{n1}, Y_{n2}, \dots, Y_{nk})' \in \mathbb{R}^n$  be a sequence of random vectors such that

$$\sqrt{n}(Y_n - \mu) \xrightarrow{d} N(0, \Sigma),$$

where  $\mu \in \mathbb{R}^k$ . Let  $g : \mathbb{R}^k \rightarrow \mathbb{R}$  have derivative  $\Delta_g(\mu)$  at  $\mu \in \mathbb{R}^k$  and derivatives are non-zero. Then,

$$\sqrt{n}(g(Y_n) - g(\mu)) \xrightarrow{d} N(0, \Delta_g(\mu)' \Sigma \Delta_g(\mu)).$$

Hence, we now require the joint distribution of  $\overline{N}_t, \overline{N}_{t+1}$  to obtain the asymptotic distribution of  $\widehat{\omega}(t)$ . It is observed that due to the increment in the time difference, the correlation between the size variables decreases. So, we consider the following joint distribution between  $\overline{N}_t, \overline{N}_{t+1}$ , and  $\overline{N}_{t+2}$  is given as

$$\begin{pmatrix} \overline{N}_t \\ \overline{N}_{t+1} \\ \overline{N}_{t+2} \end{pmatrix} \sim N_3 \left( \begin{pmatrix} \mu(t) \\ \mu(t+1) \\ \mu(t+2) \end{pmatrix}, \frac{1}{n} \begin{pmatrix} \sigma^2 & \rho\sigma^2 & \rho^2\sigma^2 \\ \rho\sigma^2 & \sigma^2 & \rho^2\sigma^2 \\ \rho\sigma^2 & \rho^2\sigma^2 & \sigma^2 \end{pmatrix} \right).$$

Let us consider  $\overline{N}(t) = U; \overline{N}(t+1) = V; \text{ and } \overline{N}(t+2) = W$ . So, the expression 25 becomes,

$$\widehat{\omega}(t) = \log \left[ \frac{\log V - \log U}{\log W - \log V} \right] = \phi(U, V, W)$$

Now, for the asymptotic distribution

$$\begin{aligned} \frac{\partial \phi}{\partial u} &= \frac{\log w - \log v}{\log v - \log u} \frac{\partial}{\partial u} \left( \frac{\log v - \log u}{\log w - \log v} \right) \\ &= \frac{1}{u \log \left( \frac{u}{v} \right)} \\ &= \frac{1}{\mu_t \log \left( \frac{\mu_t}{\mu_{t+1}} \right)} \\ &= \frac{ac}{b} \frac{1}{N_0 (e^{-a(t+1)^c} - e^{-at^c}) \exp \left[ \frac{b}{ac} (1 - e^{-at^c}) \right]} \end{aligned}$$

$$\begin{aligned} \frac{\partial \phi}{\partial v} &= \frac{\log w - \log v}{\log v - \log u} \frac{\partial}{\partial v} \left( \frac{\log v - \log u}{\log w - \log v} \right) \\ &= \frac{\frac{1}{v} \log \left( \frac{w}{u} \right)}{\log \left( \frac{v}{u} \right) \log \left( \frac{w}{v} \right)} \\ &= \frac{\frac{1}{\mu_{t+1}} \log \left( \frac{\mu_{t+2}}{\mu_t} \right)}{\log \left( \frac{\mu_{t+1}}{\mu_t} \right) \log \left( \frac{\mu_{t+2}}{\mu_{t+1}} \right)} \\ &= \frac{ac}{b} \frac{(e^{-at^c} - e^{-a(t+2)^c})}{N_0 \exp \left[ \frac{b}{ac} (1 - e^{-a(t+1)^c}) \right] (e^{-at^c} - e^{-a(t+1)^c}) (e^{-a(t+1)^c} - e^{-a(t+2)^c})} \end{aligned}$$

$$\begin{aligned} \frac{\partial \phi}{\partial w} &= \frac{\log w - \log v}{\log v - \log u} \frac{\partial}{\partial w} \left( \frac{\log v - \log u}{\log w - \log v} \right) \\ &= \frac{1}{w \log \left( \frac{v}{w} \right)} \\ &= \frac{1}{\mu_{t+2} \log \left( \frac{\mu_{t+1}}{\mu_{t+2}} \right)} \\ &= \frac{ac}{b} \frac{1}{N_0 (e^{-a(t+2)^c} - e^{-a(t+1)^c}) \exp \left[ \frac{b}{ac} (1 - e^{-a(t+2)^c}) \right]} \end{aligned}$$

Now, by applying the multivariate delta method, we obtain the distribution of  $\widehat{\omega}(t)$  for the extended Gompertz growth model, which is given as

$$\sqrt{n}(\widehat{\omega}(t) - \omega(t)) \sim N(0, \Delta' \Sigma \Delta)$$

where  $\Delta' = \left( \frac{\partial \phi}{\partial u}, \frac{\partial \phi}{\partial v}, \frac{\partial \phi}{\partial w} \right) \Big|_{\theta = \hat{\theta}}$  and  $\Sigma$  is the variance covariance matrix.

### 6 Simulation study

We will now perform the simulation experiment by considering the following growth process

$$N_t = \mu_t + \epsilon_t, \quad t = 1, 2, \dots, s. \tag{26}$$

Note that the error vector  $\epsilon_t = (\epsilon_{t1}, \epsilon_{t2}, \dots, \epsilon_{ts})'$  follows the multivariate normal distribution with **zero** mean and the dispersion matrix  $\Sigma$ . In growth studies, it is a common assumption that observations at closer time points are highly correlated, and as the time difference increases, correlations between them diminish [4, 30]. In this connection, one should opt for the covariance matrix with the Koopman structure [31], which is given by

$$\Sigma = \sigma^2 \begin{pmatrix} 1 & \rho & \dots & \rho^{s-1} \\ \rho & 1 & \dots & \rho^{s-2} \\ \vdots & \vdots & \ddots & \vdots \\ \rho^{s-1} & \rho^{s-2} & \dots & 1 \end{pmatrix}.$$

It is observed that for large  $s$ , elements away from the principal diagonal would be almost zero. It is clear that the covariance between  $N_t$  and  $N_{t+j}$  will be higher for small  $j$  and close to zero for large  $j$ . We generate the size variable  $N_t$  at  $s = 20$  time points for  $n = 20$  different individuals from multivariate normal distribution using the mean structure  $(\mu_1, \mu_2, \dots, \mu_s)$  with the aforementioned dispersion matrix. We perform the simulation experiment for the four growth equations, elaborated separately below.

### 6.1 Gompertz growth law

We use the following size model for the simulation purpose in the case of the Gompertz growth law

$$\mu_t = N_0 \exp \left[ \frac{b}{a} (1 - e^{-at}) \right] \tag{27}$$

with  $b = 1; a = 0.25; \sigma = 0.01; \rho = 0.5; N_0 = 0.1$ . The mean size and the respective RGR at 20 time points are enumerated by the formulas  $\bar{N}_t = \frac{1}{20} \sum_{i=1}^{20} N_{it}$  for  $t = 1(1)20$ , and  $\widehat{R}(t) = \log \left( \frac{N_{t+1}}{N_t} \right)$  for  $t = 1(1)19$  respectively. We also estimate the RRRGR using the estimator 25. The estimated magnitudes of the RGR and that of RRRGR are presented in Fig. 12a and b. The RGR profile in Fig. 12a shows the decreasing character, which overlaps with the Richard, Von Bertalanffy growth model, etc. But, the constant nature of RRRGR profile in Fig. 12b ensures us to capture the underlying true Gompertz growth model. Note that the solid (red) line in the figure is generated from the general estimator mentioned in the expression 25.

### 6.2 Richard growth model

We simulate the Richard growth model to obtain the size data from the following expression

$$\mu_t = K \left[ 1 + \left( \frac{1}{N_0^b} - 1 \right) e^{-brt} \right]^{-\frac{1}{b}}. \tag{28}$$

Here we consider  $b = 0.05; r = 5; \sigma = 0.0001; \rho = 0.5; N_0 = 0.1; K = 10$  to perform the experiment for 20 time points. We plot the simulated RGR and RRRGR values in Fig. 13. The decreasing fashion of the RGR (Fig. 13a) compels any experimenter to look at another measure, viz. RRRGR to capture the true model. The RRRGR profile in Fig. 13b makes it easy for anyone to conclude that the underlying growth mechanism must belong to the Richard family.

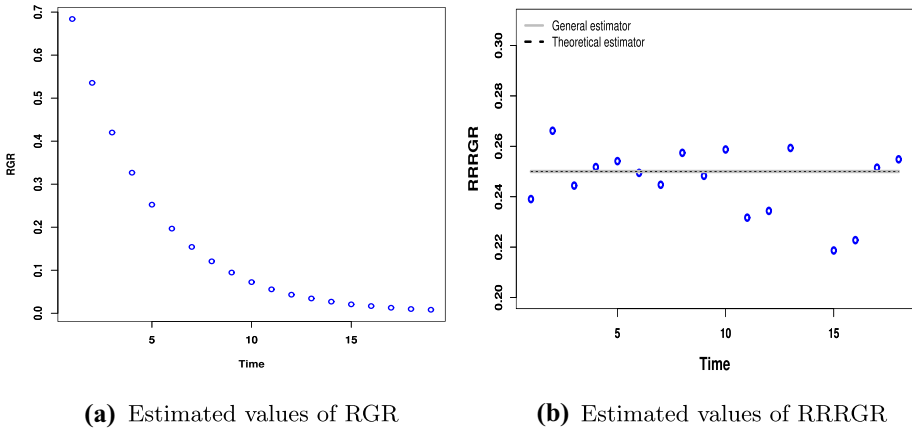


**Fig. 12** Sub-figure **a** represents the RGR over time from the simulated data from Gompertz growth model for  $b = 1, a = 0.25, \sigma = 0.01, \rho = 0.5, N_0 = 0.1$ . Sub-figure **b** depicts the general estimator of RRRGR over time for the same data

### 6.3 Extended Gompertz growth law

We generate the data of the extended Gompertz model from the following size profile

$$\mu_t = N_0 e^{\left[ \frac{b}{ac} (1 - e^{-at^c}) \right]}, \tag{29}$$

which is proposed by Chakraborty et al. [6]. Here we use  $b = 1, c = 0.5, \sigma = 0.001, \rho = 0.5; N_0 = 0.1, a = 0.5$  to simulate the growth data for 20 time points. Note that the author remarks that for  $c \leq 1$ , the fitness function should follow the decreasing pattern (see Fig. 14a). These characteristics of RGR are also being overlapped with the Richards,

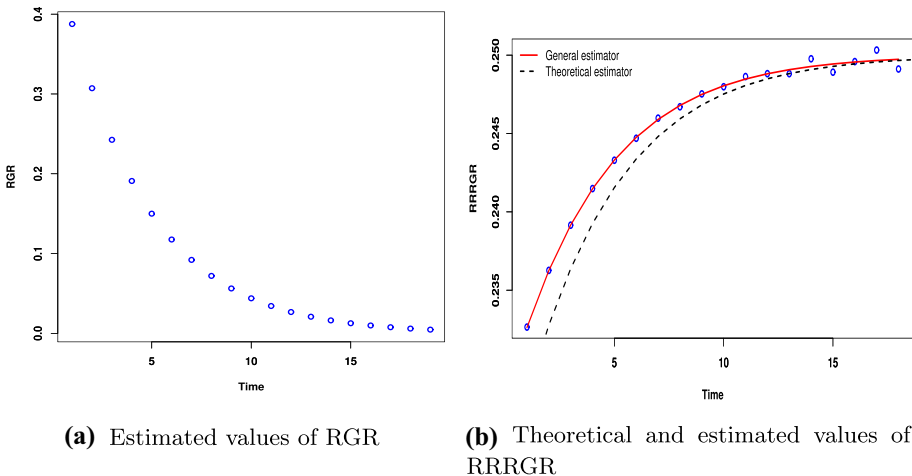


**Fig. 13** Sub-figure **a** represents the RGR over time from the simulated data from Richard growth model for  $b = 0.05, r = 5, \sigma = 0.0001, \rho = 0.5, N_0 = 0.1, K = 10$ . Sub-figure **b** depicts the empirical RRRGR over time for the same data using general estimator of RRRGR. The plot of RRRGR shows how the estimated RRRGR is close to the theoretical RRRGR

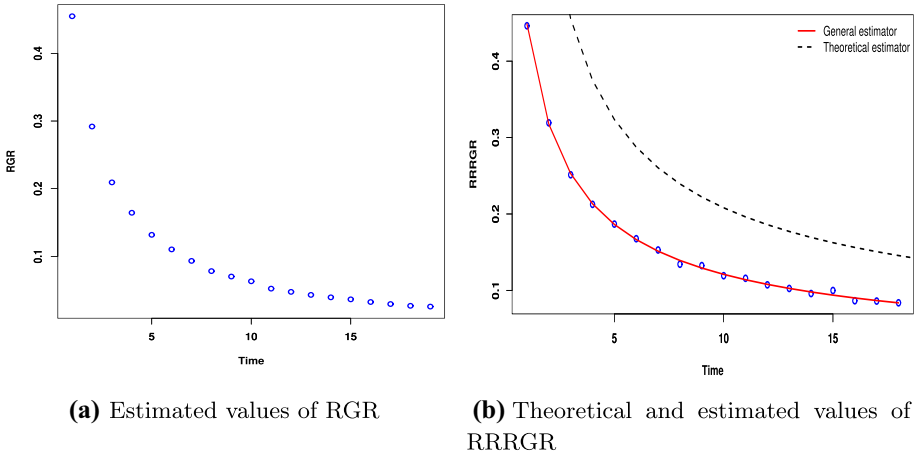


**Fig. 14** Sub-figure **a** represents the RGR over time from the simulated data from Extended Gompertz growth model for  $b = 1, c = 0.5, \sigma = 0.001, \rho = 0.5, N_0 = 0.1, a = 0.5$ . Sub-figure **b** depicts the empirical RRRGR over time for the same data using general estimator of RRRGR

Gompertz, Von Bertalanffy, etc., model. We again choose the RRRGR metric to search for the true model in this connection. The RRRGR profile in Fig. 14b depicts the decreasing pattern, which certainly excludes the Gompertz, Richard law.

### 6.4 Von-Bertalanffy law

We generate the data of the Von-Bertalanffy growth model from the following size profile

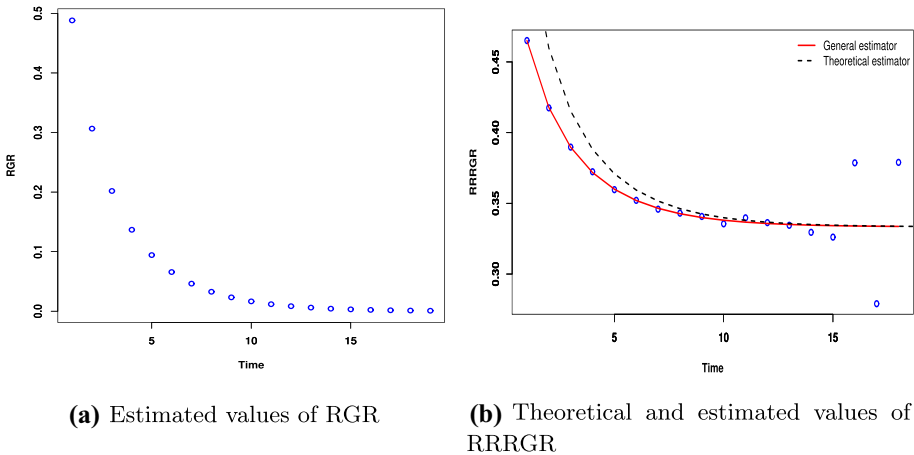


**Fig. 15** Sub-figure **a** represents the RGR over time from the simulated data from Von Bertalanffy for  $r = 1; \sigma = 0.0001; \rho = 0.5; N_0 = 0.1$ . Sub-figure **b** depicts the empirical RRRGR over time for the same data using a general estimator of RRRGR. The plot of RRRGR shows how the estimated RRRGR is close to the theoretical RRRGR

$$\mu_t = \left[ 1 - \left( 1 - N_0^{\frac{1}{3}} \right) e^{-\frac{t}{3}} \right]. \tag{30}$$

Here we consider  $r = 1; \sigma = 0.0001; \rho = 0.5; N_0 = 0.1$  to generate the size data for 20 time points. The RGR profile in Fig. 15a demonstrates the decreasing character. Figure 15b also shows that the RRRGR profile captures a decreasing trend. However, the simulation experiment in Fig. 15b shows that in the case of the Von-Bertalanffy model, the roles of the theoretical and general estimator are at par in capturing the trait of the RRRGR function, which is not for the case of the extended Gompertz law.

**Remark 7** We already mention that both the growth measures, i.e., IMR and RRRGR possess similar characteristics for specific growth laws. So, it will be difficult for any experimenter to choose the proper growth metric to identify the true growth status of any species. So, we perform a simulation experiment to compare the statistical significance between the IMR and RRRGR. In this connection, we consider the extended Gompertz model (henceforth, EGM) to pursue the whole experiment as the fitness profile of the EGM follows the non-monotonic trait. Since the RGR metric cannot provide precise growth information, we seek another growth measure between IMR and RRRGR to portray the underlying growth regulation. We presented the whole simulation work through Fig. 16a, b, and c. The diagram reflects that both the RRRGR and IMR can capture the trend of the simulated data. However, it is worth noting that the growth measure RRRGR becomes statistically more significant than the IMR when we compare both by any standard model selection criteria,

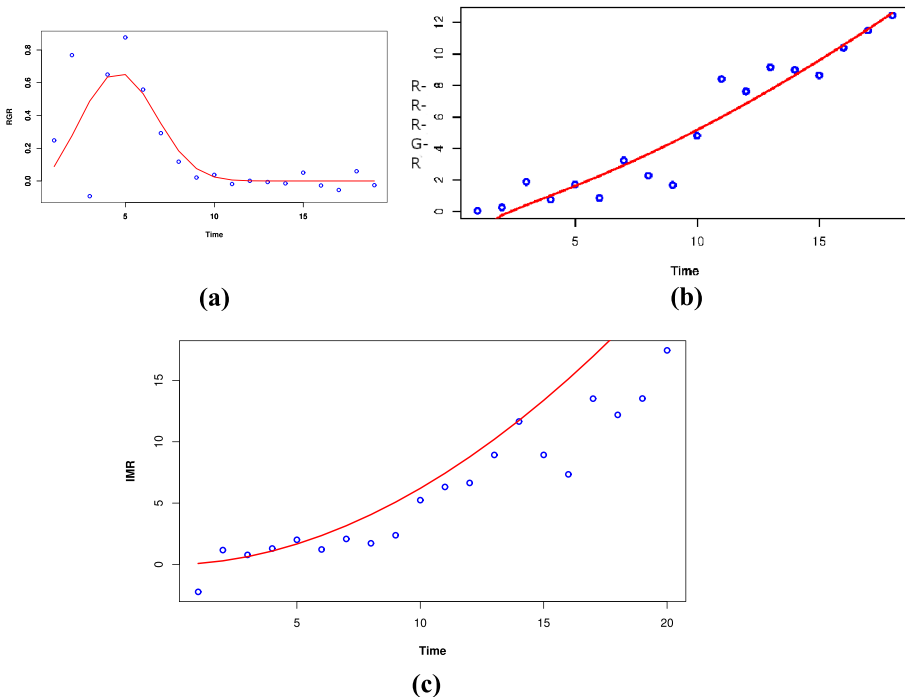


**Fig. 16** Simulation results compare three growth measures, viz. RGR, RRRGR, and IMR, by the figures (a), (b), (c) respectively. Here the observed data are presented through dots, and the solid (red) lines are the estimated curves



viz. AIC. The magnitude of AIC stands to be lower for the RRRGR metric than the IMR on the regression design, which can infer that in terms of identifying the true growth status, the efficacy of RRRGR is significantly better than the IMR.

**Remark 8** Hence, it is worthy in mentioning that IMR and RRRGR are equally significant in predicting the precise growth status of the species. But, there remains a certain distinction between the measures, which are listed below:

1. When the population size is small, there is no shortage of resources, and the species can enjoy sufficient support of food, shelter, and habitat in nature. Then, the fitness of the species is high. But, when the population reaches carrying capacity, the resource becomes exhausted. Consequently, the species fitness reduces, so the population becomes more sensitive under small perturbations. The reduction of fitness leads the population to either be in an extinction state or a chaotic regime, and the species shows unstable dynamics. Under these circumstances, the population may not return to its original size. Hence, return rate (RR) is a formidable tool for measuring the deflection rate from the species stable equilibrium density. Note that the population is not only exposed to low fitness at a specific density. Resource scarcity may occur accidentally at any intermediate population size between the minimum and maximum abundance. So, the concept and the definition of return rate can be extended to any intermediate size. Under the proposed flexible definition, we are interested in knowing the return rate's behavior for all intermediate sizes. Note that the return rate can be alternatively interpreted as the relative changes of the relative growth rate. Moreover, as this growth rate talks about the story of returning to its original size, the direction is important. The direction is incorporated through a negative sign, and hence the proposed growth rate is finally interpreted as the reverse of the relative of relative growth rate. Note that the instantaneous maturity rate (IMR) reflects the precise growth status of the species in comparison with the relative growth rate (RGR). However, IMR cannot speak about the returning guideline in the presence of uncertainties while predicting the true status of the species.
2. IMR is the seminal attempt to predict the precise growth status of the species, so its importance is undeniable. But, at the same time, IMR possesses certain limitations starting from the analytical expression. By definition, IMR is a function of carrying capacity, and hence the empirical estimate of IMR depends on the model parameter. So, IMR provides imprecise estimates if the selection of the underline model is wrong. On the contrary, the proposed measure RRRGR is independent of the model parameters.
3. It is hard to find the analytic expression of IMR in many growth models (for example, BBEGM [1], Co-operation model [25]) and hence intractable for identifying the true growth rate of species. However, it is not the case with RRRGR.
4. The RRRGR has better power in characterizing growth curves than the RGR and IMR. So, we should give more preference to the measure RRRGR as a model selection tool compared to the other growth rates. This issue is depicted in Fig. 16, where we can observe that RRRGR is a better representative for identifying the underline model BBEGM.

## 7 RRRGR modeling: a case study through deterministic and stochastic approach

In the recent study by Bhowmick and Bhattacharya [1] and Chakraborty et al. [6], it is shown that the non-monotonic fitness function could be used to model the fish growth, which was subjected to the change in the environmental condition. Bhowmick and Bhattacharya [1] considered the adaptability effect due to transferring the fish community from one environment to another. Nevertheless, Chakraborty et al. [6] use the stress properties of any fish to model their fitness profile. This would initially lead the RGR of any species to gradually increase over time, then decrease as time gradually increases, leading to a bell-shaped fitness profile. Such a non-monotonic bell-shaped structure generates the same RGR values at two distinct time points. Thus, for a given value of RGR, it is difficult for the experimenter to identify the true time points due to the many to one functional relationship of fitness. So, there is a need to seek another measure to overcome this problem of functional relationships.

Recently, Chakraborty et al. [2] proposed a new growth metric IMR to seek the species maturity. Now, we will initially use the measure IMR to provide the growth status of the species. In this connection, we consider the growth curve “BBEGM” as a test bed model [1] to demonstrate the aforementioned ecological situation. The analytical form of the growth curve is presented in Eq. 2. Now, the mathematical form of IMR for the model 2 can be obtained by the following relationship

$$m(t) = \frac{be^{-at}t^c}{\int_t^\infty be^{-au}u^c du}. \quad (31)$$

However, the closed form expression of the relation 31 is intractable for all non-integer values of  $c$ , which fails to provide a general expression of IMR for Eq. 2. The plausible reason behind this event is the non-existence of the analytical solution of the model 2. Note that Bhowmick and Bhattacharya [1] used two values of the adaptability parameter, i.e.,  $c = 1$  and  $c = 2$  for demonstrating the characteristics of the growth model 2. So, we consider  $c = 1$  to obtain the expression of IMR. The mathematical demonstration is given in the following,

$$\begin{aligned} m(t) &= \frac{bte^{-at}}{\int_t^\infty bue^{-au} du} \\ \implies m(t) &= \frac{a^2 t}{at + 1} = \frac{a^2}{a + \frac{1}{t}} \end{aligned} \quad (32)$$

The expression 32 shows that asymptotically IMR converges to the decay parameter ( $a$ ) of the function 2. The numerical experiment in Fig. 17a also illustrates that for the large time point, the species maturity status can be well explained by the decay parameter ( $a$ ). We can perform a similar kind of experiment for all integer values of adaptability parameter  $c$ . Furthermore, we believe that to explain the species growth status precisely, it is required to obtain a general formula of any metric for a specified law. Nevertheless, the manifestation of the mathematical structure for the IMR cannot be developed for the growth curve 2 due to the non-existence of a closed form solution. So, it is better to use an alternative measure that will overcome this aspect. Hence, we look to our proposed growth function “RRRGR” to provide complete growth information for the species following the BBEGM law. The analytical expression of RRRGR for the BBEGM law is presented in the first row of Table 2 in the supplementary file. The functional form suggests that asymptotically

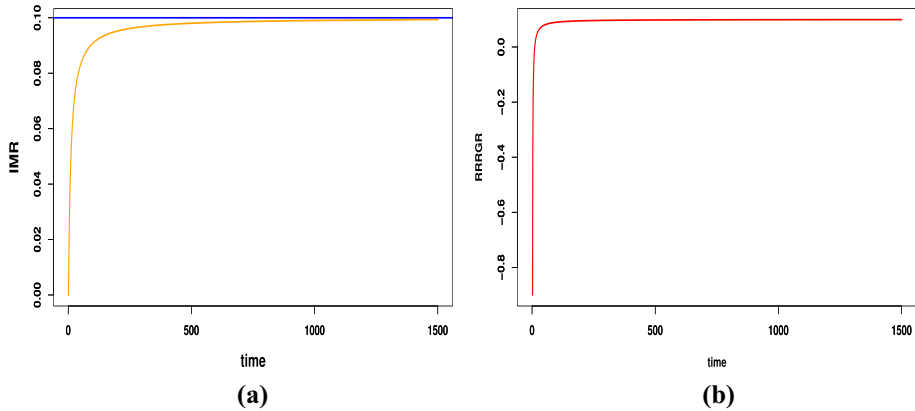


**Fig. 17** The diagram captures the trait of the **a** IMR and **b** RRRGR profile for the BBEGM [1]. Here we consider  $b = 0.01, a = 0.1, c = 1$  for generating the figures

RRRGR converges to the decay rate parameter ( $a$ ) of the model 2 (see Fig. 17b). So, we propose the following theorems to support the analytical properties of the BBEGM law to the three growth measures RGR, IMR, and RRRGR, respectively.

**Theorem 2** *If  $R(t_1) = R(t_2)$  holds for two time points  $t_1$  and  $t_2$ , then there exists one time point  $\frac{c}{a}$  such that  $t_1 < \frac{c}{a} < t_2$ , here  $R(t)$  is maximized at a point  $t = \frac{c}{a}$*

**Proof** Proof is given in the supplementary material.

**Theorem 3** *If  $m(t)$  is the IMR at time  $t$ , and two time points  $t_1$  and  $t_2$  are such that  $t_1 < \frac{c}{a} < t_2$  and  $R(t_1) = R(t_2)$ , the following relation holds for  $m(t)$ :  $m(t_1) < m(\frac{c}{a}) < m(t_2)$*

**Proof** Proof is given in the supplementary material.

**Theorem 4** *If  $\omega(t)$  is the RRRGR at time  $t$ , and two time points  $t_1$  and  $t_2$  are such that  $t_1 < \frac{c}{a} < t_2$  and  $R(t_1) = R(t_2)$ , the following relation holds for  $\omega(t)$ :  $\omega(t_1) < \omega(\frac{c}{a}) < \omega(t_2)$*

**Proof** Proof is given in the supplementary material.

### 7.1 Deterministic analog of RRRGR equation

In order to study the inherent dynamics of any natural system, it is essential to express the system through the rate equation as it can measure the change of the variable per unit of time. Consequently, one will get a complete picture of the system’s dynamics by analyzing those rate equations. So, to get the complete growth profile of any species in ecology, it will be better to nurture the rate equation than the size modeling. Here, we also construct a modeling framework through the rate of change of RRRGR instead of the negative of relative fitness equation. In this connection, we consider the BBEGM growth Eq. [1] as a test

bed model to provide precise growth information when species are subjected to the adaptability phase. The RRRGR equation for the BBEGM model is given by

$$\omega(t) = -\frac{1}{R(t)} \frac{dR(t)}{dt} \tag{33}$$

Now, differentiating both sides of the above with respect to  $t$ , we have,

$$\frac{d\omega(t)}{dt} = \frac{1}{R^2(t)} \left( \frac{dR(t)}{dt} \right)^2 - \frac{1}{R(t)} \frac{d^2R(t)}{dt^2} \tag{34}$$

Hence, from (2) and (34), we conclude that

$$\omega(t) = a - \frac{c}{t} \tag{35}$$

$$\frac{d\omega(t)}{dt} = \frac{c}{t^2} \tag{36}$$

**Remark 9** This relation (36) clearly shows that rate of change of the negative of relative fitness of the species is inversely proportional to an allometry of time i.e. when any species is the at the verge of maturity then, the adaptability power to cope up with a new environment decreases due to their low maturity.

**Remark 10** Here the constant  $c$  not only acts as an adaptability coefficient; instead, it plays the role of proportionality constant too. Note that this function is also a monotonically increasing function of time. However, the relationship 36 establishes a connection between the adaptability coefficient and the rate of change of RRRGR function of the species.

**Remark 11** The limiting form of the relation (2) leads us to the following result

$$\begin{aligned} -\frac{c}{t^2} &= -\frac{1}{R(t)} \left[ \frac{v^2(t)}{R(t)} - a_c(t) \right] \\ \implies c &= \frac{t^2}{R(t)} \left[ \frac{v^2(t)}{R(t)} - a_c(t) \right] \end{aligned} \tag{37}$$

where  $\frac{dR(t)}{dt} = v(t) =$  velocity of the RGR at time point  $t$  along with  $\frac{d^2R(t)}{dt^2} = a_c(t) =$  acceleration of the RGR at any time point  $t$ . Bhowmick and Bhattacharya [1] proposed that the species incremental effect should be captured through the positive value of  $c$ . Considering the fact, we can write that

$$\begin{aligned} \frac{v^2(t)}{R(t)} &> a_c(t) \\ \implies a_c(t) &< \frac{v^2(t)}{R(t)} \end{aligned} \tag{38}$$

The relation (38) refers that due to the adaptability to a new environment species fitness profile may change, but the hereditary tendency does not change too much. It gives a synergistic view of the relation between the centripetal acceleration and the particle’s velocity

in a non-uniform circular motion. Hence, the species which are subjected to any new habitat must have to maintain the relation (38) for their sustainability in that new environment. This implies that species always try to reach their carrying capacity for their survival prospect irrespective of the situation.

## 7.2 Stochastic model formulation

The inherent property of any species is to adapt to its new territory when they are transferred from one hoop net to another. This adaptability effect varies from one population to another as two factors govern it, one is internal, and another is the external regulator. (i) The internal responses occurred due to their hormonal oscillations, blood pressure variations, metabolic rate, enzymatic processes, cellular metabolism, or individual characteristics like body mass index and genes [6]. This will affect their cellular levels. (ii) But in comparison, the external sources of variation occur due to minor differences in the experimental procedure, dissolved oxygen, temperature, sun-light penetration, phytoplankton density, availability of food, etc. [32, 33]. Thus in the modeling framework, it is essential to incorporate the unanticipated changes in growth due to environmental fluctuations. So, we extend the proposed deterministic model 36 to its stochastic analog by introducing the concept of the stochastic differential equation (SDE), as it is known that the SDE is a natural choice to model a dynamical system that is subject to random environmental influences [34, 35]. We will compare the performance of the proposed model under this adaptability effect with the stochastic version of the other standard models. The stochastic analog of (33) can be represented by

$$d\omega(t) = f(\omega(t), t)dt + \sigma(\omega(t), t)dW(t), \quad (39)$$

where  $\{W_t, t \geq 0\}$  is standard Brownian motion,  $f(\omega(t), t)$  is called the drift coefficient, and  $\sigma(\omega(t), t)$  is the diffusion coefficient [34–36]. When any species are transferred into the new environment, individual variation between them is imminent. So the adaptability power to cope with the new environmental situation is expected to vary from one individual to the other. As a consequence, there must be significant variation in their maturity. Different individuals are exposed to the significant variation in maturity rate  $d\omega(t)$  in such a case. As a result, the variance of the maturity of an individual should be a decreasing function of age because while individuals are reaching close to their maturity, they have a small amount of variation compared to the earlier stage of growth. So  $\text{var}(d\omega(t))$  is proportional to either  $e^{-mt}$  for  $m > 0$  or with  $\frac{1}{t^p}$  depending on the specific design of the experiment. But without any loss of generality, here we consider the term  $e^{-mt}$  proportional with  $\text{var}(d\omega(t))$ . Note that  $\sigma(\omega(t), t)(> 0)$  is the intensity of environmental fluctuation. There exist many ways to consider SDE like Ito's sense [35, 36] and Stratonovich sense, but in this manuscript, we enumerate our result with the help of Ito's calculus. We take the drift coefficient from Eq. 36, then the SDE takes the following form

$$d\omega(t) = \frac{c}{t^2} + \sigma e^{-mt}dW(t). \quad (40)$$

Integrating, we get,

$$\omega(t) = \omega(t_0) + c \left( \frac{1}{t_0} - \frac{1}{t} \right) + \sigma \int_{t_0}^t e^{-mt} dW(t) \tag{41}$$

Now taking expectation on both sides of 41, we have,

$$E(\omega(t)) = m_{t_0} + c \left( \frac{1}{t_0} - \frac{1}{t} \right)$$

Here  $\omega_{t_0}$  ( $= \omega_0$ ) is a random variable with mean  $m_{t_0}$ . Now, the variance of  $\omega(t)$  governed by Eq. 41 is given by

$$\text{var}(\omega(t)) = \sigma^2 \text{var} \left( \int_{t_0}^t e^{-mt} dW(t) \right) \tag{42}$$

Using Ito’s isometry, we obtain the variance as

$$\begin{aligned} \text{var}(\omega(t)) &= \sigma^2 \text{var} \left( \int_{t_0}^t e^{-2mt} dt \right) \\ \implies \text{var}(\omega(t)) &= \frac{\sigma^2}{2m} [e^{-2mt_0} - e^{-2mt}] \end{aligned} \tag{43}$$

Therefore, considering the relation (43), the conditional distribution for BBEGM [1], i.e.,  $\omega(t(k))|\omega(t(k-1))$  follows  $N(m_1, \sigma_1)$  distribution with  $m_1 = \omega(k-1) + c \left( \frac{1}{t_{k-1}} - \frac{1}{t_k} \right)$ ,  $\sigma_1 = \frac{\sigma^2}{2m} (e^{-2mt_{k-1}} - e^{-2mt_k})$ .

Similarly, the expression for the conditional distribution of the PEGM [6], i.e.,  $\omega(t(k))|\omega(t(k-1))$  follows  $N(m_2, \sigma_2)$  distribution with  $m_2 = \omega(k-1) + (r(t_k^{c-1} - t_{k-1}^{c-1}) - (1-c) \left( \frac{1}{t_{k-1}} - \frac{1}{t_k} \right))$ ,  $\sigma_2 = \frac{\sigma^2}{2m} (e^{-2mt_{k-1}} - e^{-2mt_k})$ .

**Remark 12** The conditional distribution for BBEGM [1] with the diffusion coefficient  $1/t^p$  is  $\omega(t(k))|\omega(t(k-1))$  and follows  $N(m_3, \sigma_3)$  distribution with  $m_3 = \omega(k-1) + c \left( \frac{1}{t_{k-1}} - \frac{1}{t_k} \right)$ ,  $\sigma_3 = \frac{\sigma^2}{1-2p} \left( (t_k)^{1-2p} - (t_{k-1})^{1-2p} \right)$ .

**Remark 13** The expression for the conditional distribution of the PEGM [6] with the diffusion coefficient  $1/t^p$  is  $\omega(t(k))|\omega(t(k-1))$  and follows  $N(m_4, \sigma_4)$  distribution with  $m_4 = \omega(k-1) + \left( r(t_k^{c-1} - t_{k-1}^{c-1}) - (1-c) \left( \frac{1}{t_{k-1}} - \frac{1}{t_k} \right) \right)$ ,  $\sigma_4 = \frac{\sigma^2}{1-2p} \left( (t_k)^{1-2p} - (t_{k-1})^{1-2p} \right)$ .

### 7.3 Model validation

#### 7.3.1 Deterministic set up

Several authors [1, 5, 6] described that the fitting of the growth curve model to any data set follows two possible ways. In one way, absolute growth of any species is considered a response variable, and in the other RGR is treated as the response variable. Most of the literature [1, 5, 6, 11, 12, 37] survey reports that RGR modeling is superior to the absolute growth rate modeling due to the variability of the shape of RGR profile for different

growth laws. The inherent mechanism of any species growth is reflected through its fitness. Motivating from this fact and based on the advantage of our proposed growth measure, we treat RRRGR as a response variable to analyze our data set to the several existing time co-variate models. Since the RGR profile of our data set follows a non-monotonic, i.e., a kind of bell-shaped structure, in order to analyze the underlying model, we consider the PEGM [6], BBEGM [1] for the illustration purpose.

In general with respect to our proposed growth measure, any growth law can be expressed as

$$-\frac{1}{R(t)} \frac{dR(t)}{dt} = \omega(t) = f(t, N(t), \Theta) + \epsilon(t). \tag{44}$$

Our regression framework is carried out by following the above relation (44). Here  $\epsilon(t)$  measures the error of the process, i.e., the identically independently distributed (iid) normal random variables with zero mean and finite variance  $\sigma^2$ .  $f(t, N(t), \Theta)$  represents the underlying deterministic trend of RRRGR for the different growth laws. However,  $f(t, N(t), \Theta)$  can be explicit function of  $N(t)$  or time  $t$  depending on the several growth laws with a parameter space  $\Theta$ .

It is to be noted that both the RGR and RRRGR cannot be observed directly from any data set. So we always have to enumerate it from the given data set. Considering  $N(t_1)$  and  $N(t_2)$  as the size of any species at two different time points  $t_1$  and  $t_2$  respectively, several authors [2, 12, 15, 25] used the following relation as an estimate of the RGR

$$\widehat{R(t)} = \frac{\ln(N(t_2)) - \ln(N(t_1))}{t_2 - t_1} \tag{45}$$

Motivating from the above (45), we also used the following as an estimate of RRRGR ( $\omega(t)$ )

$$\widehat{\omega(t)} = \frac{\ln(\widehat{R(t_2)}) - \ln(\widehat{R(t_1)})}{t_2 - t_1}, \tag{46}$$

where  $R(t_1), R(t_2)$  represents the species fitness at two different time points  $t_1$  and  $t_2$  respectively. The whole estimation process is carried out through the non-linear regression set up. Here we use the Gauss-Newton type algorithm to minimize the residual sum of square, implemented in the “nls” routine of the R software [38]. The convergence of this method is highly sensitive to the initial value of the model parameters. Moreover, when data sets are short or too noisy, then non-linear least square (NLS) may sometimes fail to estimate the model parameters [25]. However, due to the small sample size and without proper assumption on the distribution of error, the estimated variances of the parameters may not be reliable (may be because of non-linearity in the model). To get the uncertainty in the parameter estimates, we follow a non-parametric type bootstrap estimation procedure for our data set. This method provides the distribution of  $\Theta$ . In order to follow the bootstrap technique, we first generate a  $B$  number of bootstrap samples where duplicate samples are also allowed. Now, we compute the parameter estimates using non-linear regression for each generated sample. Based on the bootstrap distribution we then compute the bootstrap mean of  $\widehat{\Theta}$ ,  $var(\widehat{\Theta})$  and enlist them in Tables 2, 3, and 4 as the estimate of  $\widehat{\Theta}$ .

### 7.3.2 Stochastic set up

We know that behind any natural phenomenon environment plays a key role. So it is essential to discuss the role of the environment in any experiment. In order to validate the proposed growth measure concerning our fish data in the presence of any environmental

**Table 2** Estimation of model parameters for various growth curve models on the cattle growth data. Note that the bold magnitude indicates the lowest AIC levels to identify the best models among the followings

Model	$\hat{a}$	$p$ -value	$\hat{r}$	$p$ -value	$\hat{c}$	$p$ -value	AIC
BBEGM	1.279	0.005	-	-	2.754	0.006	16.11
BBEGM ( $c = 1$ )	0.686	0.03	-	-	-	-	20.16
BBEGM ( $c = 2$ )	1.03	0.001	-	-	-	-	15.63
PEGM	-	-	0.04	0.05	2.34	0.000	<b>9.46</b>

effect, we should analyze the stochastic form of the several growth laws. Here we take BBEGM [1] as the test bed model (as discussed previously) to perform this work. Keeping this thing in mind, we already derive the distribution for the BBEGM model in Sect. 7.2. Now, the conditional log likelihood for this distribution is given by

$$L_{\omega}(c, \sigma, m) = -\frac{n}{2} \ln(2\pi) - \frac{n}{2} \ln\left(\frac{\sigma^2}{2\pi}\right) - \frac{1}{2} \sum_{k=1}^n (e^{-2mt_{k-1}} - e^{-2mt_k}) - A.$$

Note that  $A = \frac{m}{\sigma^2} \sum_{k=1}^n \frac{(\omega(k) - \omega(k-1) - c(\frac{1}{t_{k-1}} - \frac{1}{t_k}))^2}{e^{-2mt_{k-1}} - e^{-2mt_k}}$ .

Here  $n$  is the number of time points. It is to be noted that the above log-likelihood function is expressed for a single individual. The log-likelihood function for  $s$  individual is given by

$$L_{\omega_1, \omega_2, \dots, \omega_s}(c, \sigma, m) = \sum_{i=1}^s L_{\omega_i}(p), \tag{47}$$

where  $L_{\omega_i}(p)$  denotes the conditional log-likelihood function for the  $i$ -th individual. Now, the estimate of the model parameters can be found to maximize the relation (47). Since the explicit solution of the relation (47) is not available, so we use some standard numerical techniques like Nelder and Mead [39], quasi Newton [40], and conjugate gradient [41]. The numerical processes are carried out through the routine “m1e2” under the package “bml1e” routine as implemented in the R software [38].

### 7.3.3 Model selection criteria

Model selection is a procedure for identifying a model that has the best agreement with the data (called the “best model”) among a set of models. In growth curve literature, the selection of the growth model is based on some information criterion like Akaike information criterion (AIC) [42] and Bayesian information criterion (BIC). We choose the AIC as the yardstick to serve our purpose. The analytical expression for the AIC is given by

$$AIC = -2 \ln L + 2k,$$

where  $L$  is the maximized likelihood value, and  $k$  is the number of independent adjusted model parameters.

**Table 3** Estimated parameter values for various growth curve models in the location A. Note that the bold magnitude indicates the lowest AIC levels to identify the best models among the followings

Model	$\hat{a}$	$p$ -value	$\hat{r}$	$p$ -value	$\hat{c}$	$p$ -value	AIC
BBEGM	0.2449	0.4195	-	-	0.4210	0.5820	21.9571
BBEGM ( $c = 1$ )	0.414	0.055	-	-	-	-	<b>20.778</b>
BBEGM ( $c = 2$ )	0.7072	0.0129	-	-	-	-	24.6802
PEGM	-	-	0.1314	0.2817	1.3624	0.0163	21.6986



**Table 4** Estimated parameter values for various growth curve models in the location B. Note that the bold magnitude indicates the lowest AIC levels to identify the best models among the followings

Model	$\hat{a}$	$p$ -value	$\hat{r}$	$p$ -value	$\hat{c}$	$p$ -value	AIC
BBEGM	0.48	0.10	-	-	0.99	0.17	19.55
BBEGM ( $c = 1$ )	0.482	0.017	-	-	-	-	<b>17.61</b>
BBEGM ( $c = 2$ )	0.774	0.002	-	-	-	-	20.34
PEGM	-	-	0.15	0.17	1.56	0.003	19.52

### 7.4 Illustration with the real data

We consider the growth data of two species from different domains, viz. epidemiology and ecology. for the illustration purpose. The following subsections demonstrate the individual cases.

#### 7.4.1 Case-I

We consider the weight data (in kg) of the calves as the first case study. The raw data set is available in the literature of Kenward [43]. However, Karim et al. [29] also used the data set for their own research. The weight of the individual species at eleven time points over a 133-day period is recorded in the growth data. However, the animals are subjected to two treatments, i.e., treatment A and treatment B for the intestinal parasites. Here we demonstrate our analysis by considering the data of thirty (30) individuals with treatment A. The RGR profile of these individuals follows a bell-shaped structure as depicted in Fig. 18a. Moreover, the RRRGR profile is mentioned in Fig. 18b, which shows the increasing character. Since the RGR structure of the calves follows the bell-shaped structure, so, the underlying growth equation should be confined in between BBEGM [1] and PEGM laws [6]. In this connection, we compare these growth laws to find the best association with the corresponding growth data.

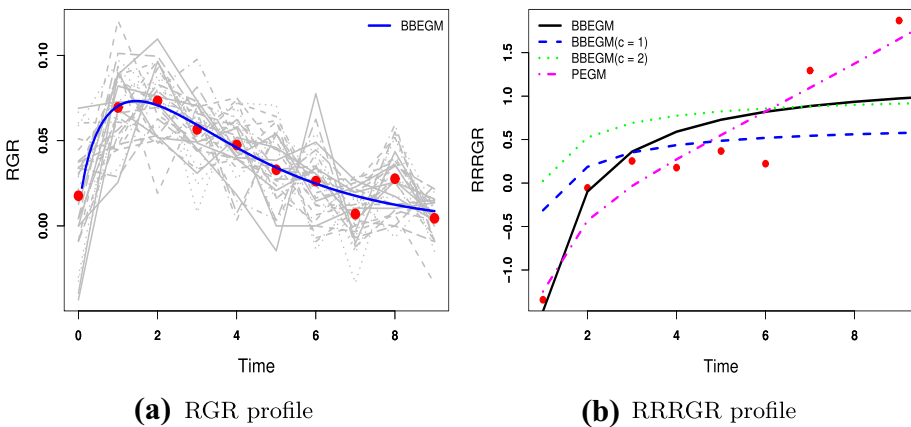


**Fig. 18** The profiles **a** and **b** represent the time-series diagram of the RGR and RRRGR function for the cattle growth data respectively. Here, both the solid and dashed lines in figure **b** are used to mention the predicted curves of the corresponding models. The name of the specified model is given in the legend of the figure

The estimated magnitudes of the model parameters are listed in Table 2. Since the magnitude of AIC for the growth model PEGM [6] stands lower among others, so it depicts that PEGM [6] has the best association with the observed data set.

#### 7.4.2 Case-II

The motivating data sets are obtained from the real-life experiment performed in the Indian Statistical Institute (ISI) pond, Kolkata. The experiment was performed to analyze the effect of water quality parameters (dissolved oxygen, temperature, etc.) on the length or size of the fish *Cirrhinus mrigala* at the different locations of the ponds. The full data sets of this experiment are presented in the thesis of [5]. Several authors [1, 2, 17, 44] also analyzed these data sets to explore their research work. Since the full experiential protocol is presented of IMR. Moreover, the simulation experiment in in the thesis of Bhattacharya [5], we provide a short glimpse of this experiment.

There were four different locations in that experimental pond, i.e., location A, location B, location C, and location D. Here we consider only first two sites, i.e., location A and location B for the illustration purpose. The length or size of the fish is recorded for twelve consecutive time points with a constant interval of times, i.e., once in a week (four times in a month). The data set consists of the “natural tip length” (the length of the fish from the lower jaw to the tip of the fork) observations of the 12 consecutive time points. At each time point, measurements of 12 randomly selected fish were recorded. Therefore, we have a longitudinal measurement of 12-time points. The parameter estimation of the deterministic models is carried out through the non-linear regression process. That stochastic set up is through the maximum likelihood technique which are elaborately discussed in Subsects. 7.3.1 and 7.3.2 respectively.

The RGR profile of the data set for the two sites, i.e., location A and B, shows the non-monotonic trait (see Fig. 20a and c). Consequently, it would be difficult for any experimenter to identify the true status of maturity of the species as the magnitudes of RGR are identical for any two distinct time points. So, we seek another new growth measure for providing a precise growth estimate of any species. The data set used here demonstrates the species growth under the adaptative environment when they are transferred from one place to another location, which is the prime reason behind the bell-shaped RGR profile. Recently, Chakraborty et al. [2] proposed a new growth metric IMR for predicting the species maturity status, where the analytical form of the measure needs substantial information about the species asymptotic size. However, it would be difficult for any experimenter to know the species carrying capacity during an experiment. In this connection, we will use the proposed alternative growth measure RRRGR to delineate the true growth status of the species. We have already mentioned in Sect. 3 that one can treat the RRRGR as the proxy for IMR. Moreover, the simulation experiment in Sect. 6 also depicts that RRRGR stands to be more statistically significant than the IMR in predicting the species actual growth status.

Note that for our data set, we empirically derive the RRRGR as the log difference of the RGR at two different time points, which is similar to the concept of RGR depicted by Fisher [3]. The time-series profile of the RRRGR in Fig. 20b and d displays an increasing character, which indicates that the underlying growth model may be the logistic, theta-logistic, extended Gompertz, etc. Since the fitness profiles of our data set follow the non-monotonic trend, we can exclude the logistic family as their size-RGR relationship follows the decreasing character. Consequently, we select the growth models of the

**Table 5** The estimated magnitudes of the model parameters for distinct growth functions analogous with the stochastic differential equation in the location A. Note that the bold magnitude indicates the lowest AIC levels to identify the best models among the followings

Model	$\hat{r}$	<i>p</i> -value	$\hat{c}$	<i>p</i> -value	$\hat{\sigma}$	<i>p</i> -value	$\hat{m}$	<i>p</i> -value	AIC
BBEGM	-	-	0.2	0.000	0.6	0.000	0.33	0.000	42.5
BBEGM ( <i>c</i> = 1)	-	-	-	-	1.17	0.0012	0.06	0.02	<b>38.5</b>
BBEGM ( <i>c</i> = 2)	-	-	-	-	1.29	0.001	0.07	0.02	39.6
PEGM	18.8	0.000	0.993	0.000	1.09	0.0014	0.59	0.03	41.7

extended Gompertz family, viz. *BBEGM* and *PEGM* for the regression purpose of predicting the species inherent growth mechanism. Here we carried out the regression work on both the deterministic and stochastic situations. The detailed process of the regression work is presented in Subsects. 7.3.1 and 7.3.2. The output of the regression work demonstrates that in both locations A and B, the growth model *BBEGM* (*c* = 1) shows the best association with the data sets among the considered models. Here we select the best model based on the AIC magnitude as mentioned in the Subsect. 7.3.3. The parameter estimates, along with the AIC values for both the deterministic and stochastic cases, are listed in Tables 3, 4, 5, and 6.

**Remark 14** The empirical study of Bhowmick and Bhattacharya [1] reveals that the *BBEGM*(*c* = 2) gives a better parameter estimation to capture the underlying growth trend of the fish for location A in comparison to the other existing growth models to the *R*<sup>2</sup>, *RMSE*, AIC, etc. Bhowmick and Bhattacharya [1] confined their whole discussion between the parametric value *c* = 1 and *c* = 2 in *BBEGM*. This would insist them to select the better model between these two based on some statistical measure like AIC. It is worthy to note that Chakraborty et al. [6] also nurture this data set in order to judge whether *PEGM* gives a better parameter estimation or not. The author shows that among the existing time co-variate models, including *BBEGM* (*c* = 1 and *c* = 2), *PEGM* gives a better estimate of AIC. Thus, AIC should play a key role in commenting on the fitness of any model. However, in our case, we find that the magnitudes of AIC for the four models, i.e., *BBEGM*, *BBEGM*(*c* = 1), *BBEGM*(*c* = 2), *PEGM*, are pretty close to each other. In this connection, we perform the bootstrap analysis to generate the bootstrap distribution of the AIC for these four models. Now, we numerically estimate the density by the Kernel density function “density” as implemented in the R software [38], which is depicted in Fig. 19. Hence, it is clear from the figure that the means of this bootstrap distribution for the four models do not differ too much. This trait ensures that the response of all the four models toward the fish data is pretty similar.

**Table 6** The estimated magnitudes of the model parameters for distinct growth functions analogous with the stochastic differential equation in the location B. Note that the bold magnitude indicates the lowest AIC levels to identify the best models among the followings

Model	$\hat{r}$	<i>p</i> -value	$\hat{c}$	<i>p</i> -value	$\hat{\sigma}$	<i>p</i> -value	$\hat{m}$	<i>p</i> -value	AIC
BBEGM ( <i>c</i> = 1)	-	-	-	-	0.96	0.0014	0.07	0.03	<b>33.6</b>
BBEGM ( <i>c</i> = 2)	-	-	-	-	1.04	0.0012	0.07	0.02	34.4
PEGM	9.63	0.000	1.03	0.000	0.95	0.0015	0.07	0.03	37.4

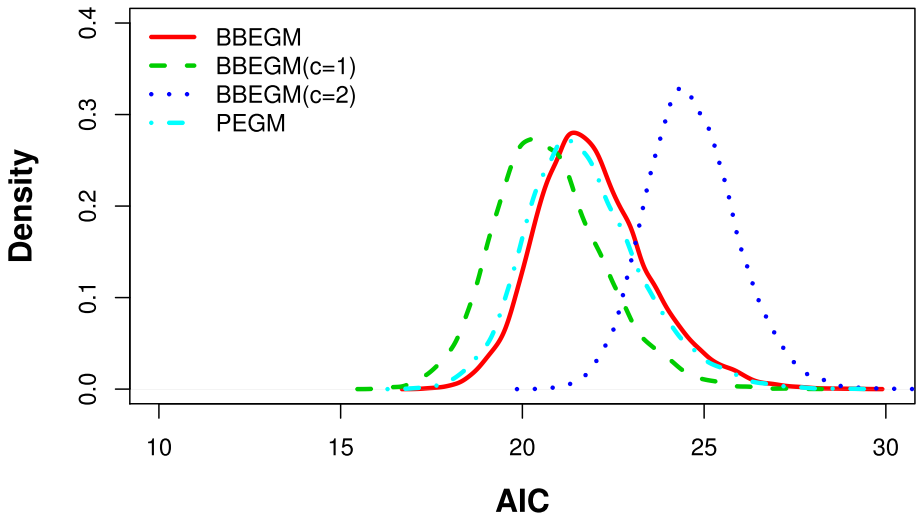
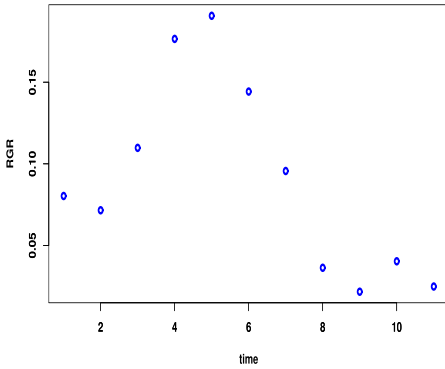


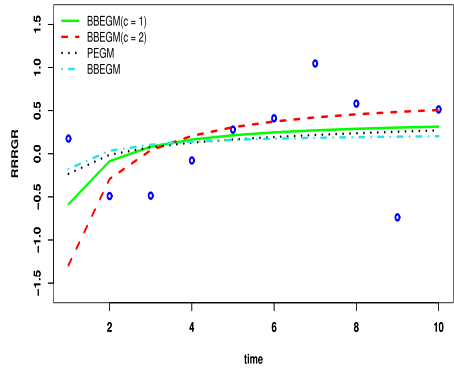
**Fig. 19** The bootstrap distribution of the AIC for BBEGM, BBEGM ( $c = 1$ ), BBEGM ( $c = 2$ ), and PEGM for location A over 1000 bootstrap samples. The density function is enumerated through the Kernel density function “density” as implemented in the R software [38]. It is quite clear from the figure that the means of this bootstrap distribution for BBEGM ( $c = 1$ ), BBEGM ( $c = 2$ ), and BBEGM do not differ too much. This trait ensures that the response of all those three models towards our fish data is almost similar

Since the RRRGR is treated as the proxy for the IMR, so we can classify the prediction process into two buckets from the perspective of the species maturity. The first classification predicts the magnitude of the negative of relative fitness of any species at any specific time point by which one can easily draw the inference on the species maturity without using the metric IMR (see Fig. 20b, d). For example, in our data sets, the species will attain its matured stage when the magnitude of the RRRGR becomes identical with the estimated values of the decay parameter, i.e.,  $\hat{a}$  both in the stochastic and deterministic process. Moreover, we also describe in Sect. 3 that the RGR-RRRGR relationship for the bell-shaped fitness profile possesses specific characteristics of having two distinct magnitudes of RRRGR for a specific RGR value. Note that these magnitudes of RRRGR represent two distinct states of the species life cycle, i.e., the infant and matured stages.

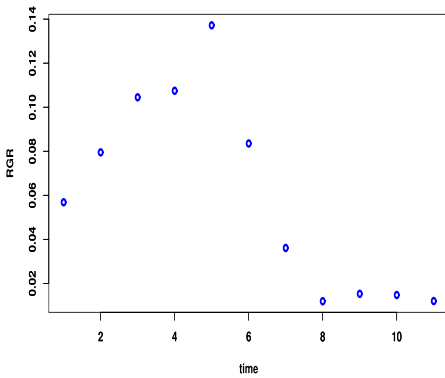
Consequently, it will be easy for an experimenter to draw the inference on the species maturity by studying the RGR-RRRGR profile, which is depicted in Fig. 21a, b. Moreover, the entire regression work also provides an estimate of the species return rate by  $0.414 \text{ time}^{-1}$  and  $0.482 \text{ time}^{-1}$  for locations A and B, respectively, which plays a crucial role in maintaining stability in the ecosystem. So, in a nutshell, we observe that the proposed measure RRRGR not only addresses the species maturity status but also provides prime information on the species return rate.



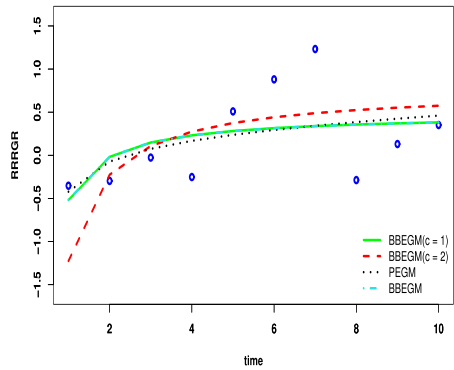
(a) RGR profile at Location A



(b) RRRGR profile at Location A

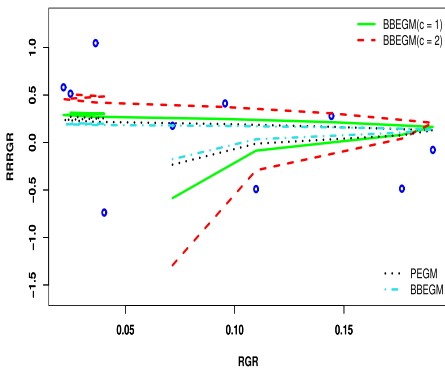


(c) RGR profile at Location B

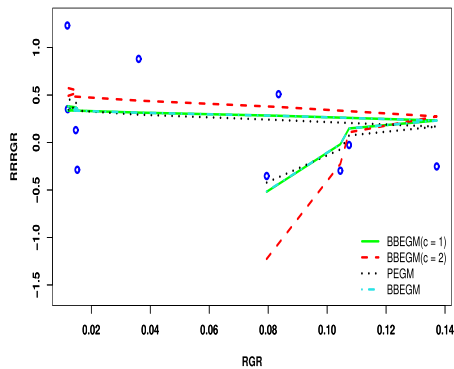


(d) RRRGR profile at Location B

**Fig. 20** The profile (a), (c) and (b), (d) represents the time-series diagram of the RGR and RRRGR for the fish data respectively. Here, both the solid and dashed lines are used to mention the predicted curves of the corresponding models. The name of the specified model is present in the legend of the figure



(a) Location A



(b) Location B

**Fig. 21** The profile (a), (b) represents the relation between the RRRGR and RGR of the fish data. Here, both the solid and dashed lines are used to mention the predicted curves of the corresponding models. The name of the specified model is presented in the legend of the figure

## 8 Conclusion

Several studies suggest that the most popular growth metric to capture the species fitness is the relative growth rate (henceforth, RGR) which is superior to the size modeling. Since then, RGR has been predominantly used in the statistical inference of growth models. The different growth laws, such as exponential, logistic, Gompertz, power, and generalized Gompertz or generalized logistic, can be characterized based on the monotonic behavior of the relative growth rate (RGR) to size or time. Thus, in this case, species fitness can be determined indeed through RGR. However, in nature, RGR is often non-monotonic and specifically bell-shaped [1, 29]. In this case, species may experience with the same fitness (RGR) for two different time points. The species precise growth and maturity status cannot be determined from this RGR function. The instantaneous maturity rate (IMR), as proposed by Chakraborty et al. [2], helps to determine the correct maturity status of the species. Nevertheless, IMR is intractable for all non-integer values of a specific parameter. Moreover, it is a function of the carrying capacity parameter unknown to any experimenter. The structural form of the metric IMR lacks the concept of species return rate, which is an essential tool in measuring species stability. In this connection, we propose the RRRGR as a proxy for the IMR. Although IMR and RRRGR possess similar mathematical property, the proposed measure RRRGR is free from the model parameters. So, the metric RRRGR will be helpful in predicting the accurate growth status of any species in compare with the IMR. Hence, the utility of the proposed measure is explained by real life data. We believe that this study would be helpful for fishery biologists in regulating the favorable conditions of growth so that the species can reach its carrying capacity with optimum effort.

**Supplementary information** The online version contains supplementary material available at <https://doi.org/10.1007/s10867-023-09628-0>.

**Acknowledgements** The author Ayan Paul is thankful to the Department of Science and Technology, Government of India, i.e., DST-INSPIRE (Grant Number: IF180793), for supporting the fellowship. We must acknowledge Md Aktar UI Karim, CSIR Senior Research Fellow from Institute of Chemical Technology, India, and Selim Reja, UGC Senior Research Fellow from the Indian Statistical Institute, Kolkata, for the technical help in preparing the revised version of the manuscript. We are also thankful to Dr. Soumalya Mukhopadhyay, Dr. Amiya Ranjan Bhowmick, Dr. Biman Chakraborty from the Visva-Bharati University, Institute of Chemical Technology, the Aliah University of India, respectively, and the anonymous reviewers for their valuable suggestions to improve the quality of the manuscript.

**Funding** The author Ayan Paul is thankful to the Department of Science and Technology, Government of India, i.e., DST-INSPIRE (Grant Number: IF180793), for supporting the fellowship.

## Declarations

**Ethical approval** The study is purely theoretical and does not involve any experiment with animals that would require ethical approval.

**Informed consent** The study does not involve any participants that would have to give their informed consent.

**Conflict of interest** The authors declare no competing interests.

## References

1. Bhowmick, A.R., Bhattacharya, S.: A new growth curve model for biological growth: some inferential studies on the growth of *Cirrhinus mrigala*. *Math. Biosci.* **254**, 28–41 (2014)

2. Chakraborty, B., Bhowmick, A.R., Chattopadhyay, J., Bhattacharya, S.: Instantaneous maturity rate: a novel and compact characterization of biological growth curve models. *J. Biol. Phys.* **48**(3), 295–319 (2022)
3. Fisher, R.A.: Some remarks on the methods formulated in a recent article on “the quantitative analysis of plant growth”. *Ann. Biol.* **7**(4), 367–372 (1921)
4. Pal, A., Bhowmick, A.R., Yeasmin, F., Bhattacharya, S.: Evolution of model specific relative growth rate: its genesis and performance over Fisher’s growth rates. *J. Theor. Biol.* **444**, 11–27 (2018)
5. Bhattacharya, S.: Growth curve modelling and optimality search incorporating chronobiological and directional issues for an Indian major carp *Cirrhinus mrigala*. Ph.D Dissertation, Jadavpur University, Kolkata, India (2003)
6. Chakraborty, B., Bhowmick, A.R., Chattopadhyay, J., Bhattacharya, S.: Physiological responses of fish under environmental stress and extension of growth (curve) models. *Ecol. Model.* **363**, 172–186 (2017)
7. Verhulst, P.-F.: Notice sur la loi que la population suit dans son accroissement. *Corresp. Math. Phys.* **10**, 113–126 (1838)
8. Gompertz, B.: On the nature of the function expressive of the law of human mortality, and on a new mode of determining the value of life contingencies. In a Letter to Francis Baily ESQ. F.R.S. &c. *Philos. Trans. R. Soc.* **115**, 513–583 (1825)
9. Richards, F.: A flexible growth function for empirical use. *J. Exp. Bot.* **10**(2), 290–301 (1959)
10. Tsoularis, A., Wallace, J.: Analysis of logistic growth models. *Math. Biosci.* **179**(1), 21–55 (2002)
11. Kundu, S., Dasgupta, N., Chakraborty, B., Paul, A., Ray, S., Bhattacharya, S.: Growth acceleration is the key for identifying the most favorable food concentration of *Artemia* sp. *Ecol. Model.* **455**, 109639 (2021)
12. Paul, A., Reja, S., Kundu, S., Bhattacharya, S.: COVID-19 pandemic models revisited with a new proposal: plenty of epidemiological models outcast the simple population dynamics solution. *Chaos Solitons Fract.* **144**, 110697 (2021)
13. Paul, A., Ghosh, N., Bhattacharya, S.: Estimation of the present status of the species based on the theoretical bounds of environmental noise intensity: an illustration through a big abundance data and simulation. *Theor. Ecol.* **15** (3), 245–266 (2022)
14. May, R., Conway, G., Hassell, M., Southwood, T.: Time delays, density-dependence and single-species oscillations. *J. Anim. Ecol.* **747–770** (1974)
15. Bhowmick, A. R., Sardar, T., Bhattacharya, S.: Estimation of growth regulation in natural populations by extended family of growth curve models with fractional order derivative: case studies from the global population dynamics database. *Ecol. Inform.* **53**, 100980 (2019)
16. Sibly, R.M., Barker, D., Hone, J., Pagel, M.: On the stability of populations of mammals, birds, fish and insects. *Ecol. Lett.* **10**(10), 970–976 (2007)
17. Chakraborty, B., Bhowmick, A.R., Chattopadhyay, J., Bhattacharya, S.: A novel unification method to characterize a broad class of growth curve models using relative growth rate. *Bull. Math. Biol.* **81**(7), 2529–2552 (2019)
18. Generalized two-parameter equation of growth: Marusic, B. Z., M. J. *Math. Anal. Appl.* **179**, 446–462 (1993)
19. Bertalanffy, L.V.: In *Fundamental Aspects of Normal and Malignant Growth*, pp. 137–259. W.W. Nowinski edn. Amsterdam (1960)
20. Bertalanffy, L.V.: Logistic growth rate functions. *J. Theor. Biol.* **21**, 42 (1968)
21. Turner, Jr., Bradely, Jr., Kirk, K.A., Pruitt, K.M.: A theory of growth. *Math. Biosci.* **29**, 367–373 (1976)
22. Korf, V.: Contribution to mathematical definition of the law of stand volume growth. *Lesnicka Prace* **18**, 339–379 (1939)
23. Koya, P.R., Goshu, A.T.: Generalized mathematical model for biological growths. *Op. J. Model. Simul.* **1**, 42–53 (2013)
24. Weibull, W.: A statistical distribution function of wide applicability. *J. Appl. Mech.* **18**, 293–297 (1951)
25. Bhowmick, A.R., Saha, B., Chattopadhyay, J., Ray, S., Bhattacharya, S.: Cooperation in species: interplay of population regulation and extinction through global population dynamics database. *Ecol. Model.* **312**, 150–165 (2015)
26. Allee, W.C.: Co-operation among animals. *Am. J. Sociol.* **37**(3), 386–398 (1931)
27. Saha, B., Bhowmick, A.R., Chattopadhyay, J., Bhattacharya, S.: On the evidence of an Allee effect in herring populations and consequences for population survival: a model-based study. *Ecol. Model.* **250**, 72–80 (2013)
28. Wasserman, L.: In: *Bayesian Inference*, pp. 175–192. Springer (2004)
29. Karim, M.A.U., Bhagat, S.R., Bhowmick, A.R.: Empirical detection of parameter variation in growth curve models using interval specific estimators. *Chaos Solitons Fract.* **157**, 111902 (2022)
30. Mukhopadhyay, S., Hazra, A., Bhowmick, A.R., Bhattacharya, S.: On comparison of relative growth rates under different environmental conditions with application to biological data. *Metron* **74**(3), 311–337 (2016)

31. Koopmans, T.: Serial correlation and quadratic forms in normal variables. *Ann. Math. Stat.* **13**(1), 14–33 (1942)
32. Barton, B.: Stress in fishes: a diversity of responses with particular reference to changes in circulating cortico steroids. *Integr. Comp. Biol.* **42**, 517–525 (2002)
33. Ditlevsen, S., Samson, A.: In *Stochastic Biomathematical Models with Applications to Neuronal Modeling*. Springer (2013)
34. Bishwal, J.: Parameter estimation in stochastic differential equations. *Evol. Appl.* (2008)
35. Allen, L. : *An Introduction to Stochastic Processes with Applications to Biology*, 2nd edn. Chapman and Hall/CRC (2010)
36. Oksendal, B.: *Stochastic Differential Equations: An Introduction with Applications*, 6th edn. Springer (2003)
37. Sau, A., Saha, B., Bhattacharya, S.: An extended stochastic Allee model with harvesting and the risk of extinction of the herring population. *J. Theor. Biol.* **503**, 110375 (2020)
38. R Core Team: R: a language and environment for statistical computing. R Foundation for Statistical Computing, Vienna, Austria (2022). <https://www.R-project.org/>
39. Nelder, J.A., Mead, R.: A simplex method for function minimization. *Computer J.* **7**, 308–313 (1965)
40. Broyden, C.G.: *Numerical Methods for Unconstrained Optimization*. Academic Press (1972)
41. Polyak, B.T.: *Introduction to optimization*. Optimization Software Inc., Publications Division, New York **1**, 32 (1987)
42. Akaike, H.: A new look at the statistical model identification. *IEEE Trans. Aut. Contr.* **19**, 716–723 (1974)
43. Kenward, M.G.: A method for comparing profiles of repeated measurements. *J. R. Stat. Soc. Ser. C Appl. Stat.* **36**(3), 296–308 (1987)
44. Roy, T., Ghosh, S., Bhattacharya, S.: A new growth curve model portraying the stress response regulation of fish: illustration through particle motion and real data. *Ecol. Model.* **470**, 109999 (2022)

**Publisher's Note** Springer Nature remains neutral with regard to jurisdictional claims in published maps and institutional affiliations.

Springer Nature or its licensor (e.g. a society or other partner) holds exclusive rights to this article under a publishing agreement with the author(s) or other rightsholder(s); author self-archiving of the accepted manuscript version of this article is solely governed by the terms of such publishing agreement and applicable law.

## Authors and Affiliations

Ayan Paul<sup>1</sup> · Neelakshi Chatterjee<sup>2</sup> · Sabyasachi Bhattacharya<sup>1</sup> 

Ayan Paul  
ayaninspire@gmail.com

Neelakshi Chatterjee  
neelakshi.chatto@gmail.com

<sup>1</sup> Agricultural and Ecological Research Unit, Indian Statistical Institute, 203, B. T. Road, Kolkata 700108, India

<sup>2</sup> Department of Mathematical Sciences, University of Cincinnati, 2600 Clifton Ave, Cincinnati, OH 45221, USA